DOI: 10.1002/adma.((please add manuscript number))

Engineering Hydrogels for Biofabrication

By *Jos Malda**, *Jetze Visser*, *Ferry P. Melchels*, *Tomasz Jüngst*, *Wim E. Hennink*, *Wouter J.A. Dhert*, *Jürgen Groll*, and *Dietmar W. Hutmacher**

Dr. J. Malda, Mr. J. Visser, Dr. F.P. Melchels, Prof. W.J.A. Dhert
Department of Orthopaedics, University Medical Center Utrecht, P.O. Box 85500, 3508 GA Utrecht (The Netherlands)
E-mail: (j.malda@umcutrecht.nl)

Dr. J. Malda, Dr. F.P. Melchels, Prof. D.W. Hutmacher
Institute of Health and Biomedical Innovation, Queensland University of Technology, Kelvin Grove Urban Village, Brisbane QLD 4059 (Australia)
E-mail: (dietmar.hutmacher@qut.edu.au)

Dr. J. Malda, Prof. W.J.A. Dhert
Department of Equine Sciences, Faculty of Veterinary Sciences, Utrecht University, Yalelaan 112, 3584 CM Utrecht (The Netherlands)

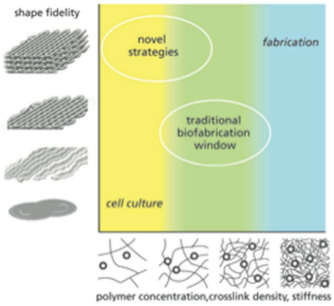

Prof. W.E. Hennink
Department of Pharmaceutics, Utrecht University, P.O. Box 80082, 3508 TB Utrecht (The Netherlands)

Mr. T. Jüngst, Prof. J. Groll
Department of Functional Materials in Medicine and Dentistry, University of Würzburg, Pleicherwall 2, 97070 Würzburg (Germany)

Prof. D.W. Hutmacher
Institute of Advanced Studies, Technical University Munich
Lichtenbergerstr. 34, 80678 Munich, Germany

Keywords: (bioprinting, biofabrication, additive manufacturing, hydrogel, biomaterials, biopolymers)

Abstract

With advances in tissue engineering, the possibility of regenerating injured tissue or failing organs has become a realistic prospect for the first time in medical history. Tissue engineering – the combination of bioactive materials with cells to generate engineered constructs that functionally replace lost and/or damaged tissue – is a major strategy to achieve this goal. One facet of tissue engineering is biofabrication, where three-dimensional tissue-like structures composed of biomaterials and cells in a single manufacturing procedure are generated. Cell-laden hydrogels are commonly used in biofabrication and are termed “bio-inks”. Hydrogels are particularly attractive for biofabrication as they recapitulate several features of the natural extracellular matrix and allow cell encapsulation in a highly hydrated mechanically supportive three-dimensional environment. Additionally, they allow for efficient and homogeneous cell seeding, can provide biologically-relevant chemical and physical signals and can be formed in various shapes and biomechanical characteristics. However, while advances in modifying hydrogels for enhanced bioactivation, cell survival and tissue formation, little attention has so far been paid to optimize hydrogels for the physico-chemical demands of the biofabrication process. The resulting lack of hydrogel bioinks have been identified as one major hurdle for a more rapid progress of the field. In this review we summarize and focus on the deposition process, the parameters and demands of hydrogels in biofabrication, with special attention to robotic dispensing as an approach that generates constructs of clinically relevant dimensions. We aim to highlight this current lack of effectual hydrogels within biofabrication and initiate new ideas and developments in the design and tailoring of hydrogels. The successful development of a “printable” hydrogel that support cell adhesion, migration and differentiation will significantly advance this exciting and promising approach for tissue engineering.

1. Introduction

Tissue engineering (TE) aims for the full restoration of damaged or degenerated tissues and organs through the use of TE, cell and growth factor delivery. Tissue-engineered constructs will have to mimic a certain degree of the native complexity of the tissue in order to assist in restoration of the full structure and functionality of the tissue. Traditionally, the three main components of TE are cells, scaffolds and growth factors and they are combined to form a construct that can be immediately implanted or incubated *in vitro* prior to implantation. A scaffold can successfully deliver cells and/or growth factors to a damaged or degenerated tissue or organ, while simultaneously providing temporal mechanical support for the period the newly formed tissue matures. However, the three-dimensional (3D) constructs that have been generated for these scaffold-based or scaffold-guided TE approaches are typically based on the random distribution of cells, matrix, and bioactive cues, since their manufacturing does not allow the control of specific distribution. Mimicking the biological and functional organizational complexity of native tissues is now regarded as the next challenge in the full regeneration of tissues.

To address this challenge, additive manufacturing (AM) technology has been employed to generate bio-engineered 3D structures to replicate the complex nature of tissue.[1] In this approach, termed "biofabrication",[2, 3] biological structures for TE, pharmacokinetic or basic cell biology studies (including disease models) are created by an computer-aided manufacturing process for patterning and assembling living and non-living materials with a prescribed 3D organization.[4] The resulting shape can be customized, and include open inner structures that improve the supply of nutrients towards embedded cells.[5] Moreover, the fabricated structures can be used to study interactions between different cells and/or bioactive compounds,[6] but could also lead to functional tissue equivalents,[7] and potentially, to whole functioning organs.[8] Recent investigations have, for example, adopted biofabrication for the

engineering of 3D constructs with the organizational features of different tissues, including skin,[9, 10] meniscus,[11] aortic valves,[12] cartilage,[13, 14] bone,[15] and blood vessels.[16]

Whilst AM technologies, as applied in the processing of metals, ceramics and thermoplastic polymers have inspired the field of biofabrication, these "classic" AM approaches generally involve the use of organic solvents, high temperatures or crosslinking agents that are not compatible with living cells and/or bioactive proteins. Hydrogels can be processes under more cell friendly conditions and often classified in the biofabrication field as "bioinks". From a biological point of view, high water content hydrogels are attractive candidates for the incorporation of cells and bioactive compounds, because they can provide an instructive, aqueous 3D environment, simulating the natural extracellular matrix.[15]

Historically, hydrogels used in tissue engineering applications are predominantly based on naturally derived polymers, including alginate, gelatin, collagen, chitosan, fibrin and hyaluronic acid.[19-21] Cells benefit from the abundance of chemical signals present in these hydrogels, resulting in high viability and proliferation rates.[19, 22] These signals can also be used to induce the formation of specific neo-tissues,[19, 20, 23] however, due to batch-to-batch variation and the sensitivity of cells (especially stem cells) to these variations, reproducibility of constructs often remains complicated. In addition, implementation of these materials in biofabrication can be challenging due to their variable printability.

In contrast to hydrogels based on natural polymers, 3D printed structures with high shape fidelity can be obtained with polymers based on synthetic networks, like poly(ethylene glycol)[24] and pluronics[25-27]. However, these hydrogels provide embedded cells with an inert environment without active binding sites,[28] often resulting in low cell viability.[25-27] In order to improve control over cellular differentiation in these gels, bioactive compounds have to be added or grafted to the network, like peptide sequences[29] and growth factors.[20, 30] Peptide

sequences can modulate cellular behavior by providing binding sites in otherwise inert hydrogels,[31] whereas growth factors can further direct cellular differentiation in order to regenerate a specific tissue type. There already are a number of reviews on the mandatory biological characteristics of hydrogels for biomedical applications and this goes beyond the scope of this review. For further reading we recommend recent reviews by Seliktar[22] and by DeForest and Anseth[28].

The present review will focus on the physicochemical aspects important for the development and characterization of hydrogels for biofabrication. Despite the fact that photocuring methods, such as two-photon polymerization[32] and stereolithograpy[33] can also yield organized 3D cell-laden hydrogel structures, their working principles do not involve deposition of gels and cells and hence pose different demands regarding hydrogel properties. Therefore, these techniques fall outside the scope of the current review. Here, we guide the reader in making choices regarding available approaches to tailor existing hydrogel platforms by means of physicochemical modification. Finally, current developments in hydrogels that could impact on the composition and properties of future hydrogel bioinks will be discussed.

2. The Biofabrication Window

Although major progress has been made with both natural and synthetic hydrogels in biofabrication,[34] bioinks have some significant complications regarding the required physical and biological properties. The central problem is that the fabrication of complex, tissue-like structures with high resolution dictates narrow boundaries for the physical properties of the hydrogels. Adittionally, the hydrogel construct should facilitate migration, proliferation and differentiation of the embedded and endogenous cells. Thereby, biofabrication imposes opposing requirements on the properties of materials and specifically the lack of such versatile hydrogel systems has been coined as an important factor restraining further progress

in this field.[1, 8, 35, 36-38] The traditional approach to improve printability of hydrogels has been increasing the polymer concentration or crosslink density.[39, 40] Highly crosslinked hydrogels serve as a stiff construction material as represented by the blue fabrication window (**Fig. 1)**. On the contrary, cells thrive best in an aqueous environment, in which their migration and matrix deposition is not limited by a dense polymer network,[28] represented by the yellow cell culture window (Fig. 1). Unfortunately, hydrogels with a low extend of crosslinks lack the ability to maintain their imposed shape on fabrication, resulting in a low shape-fidelity and limited overall mechanical properties. Therefore, most constructs have been fabricated with a moderate degree of hydrogel crosslink densities, represented by the green "traditional" biofabrication window (Fig. 1). However, since hydrogels which fit in this window compromise on biological, as well as fabrication properties, there is a need to shift this biofabrication window in order to achieve high shape-fidelity with hydrogels that facilitate maximal cell and tissue compatibility ("novel strategies" (Fig. 1)).

Hydrogels for biofabrication should allow the translation of the computer-aided design (CAD) to a tissue construct that potentially contains intricate internal and/or external organizational structures. This requires a high degree of control over the deposition process, which is closely associated with the printability of the hydrogel. The printing of inks on paper is well documented with various available tests that are taking in account surface and structural properties of the paper, however quantification of printability of ink on paper remains difficult.[41] Standardized tests to evaluate the capacity of hydrogels to be printed do not yet exist. Obviously, an important outcome parameter from a physical point of view would be the geometric accuracy or shape fidelity of the generated constructs. As such, there is a strong need for methods of geometry comparison of tissue-engineered constructs that go beyond simple visual inspection, manual measurements using rulers or calipers[42] and photographs.[11, 40, 43] Optical methods have been developed to assess the geometric fidelities of tissue

constructs using laser triangulation.[42] Although this yields valuable data on the outer contours of homogeneous solid tissue replacements, such as for the meniscus, this technique will not visualize the potentially more intricate internal geometry. More recently, Murphy *et al*.[10] evaluated properties relevant to bioprinting, including printability, of a range of available hydrogels. In an attempt to quantify the printability, deviation of a 1.0 x 1.0 cm printed square area was determined. Although the authors were challenged by the fact that not all hydrogels could be reproducibly processed by the printer, this allowed for an, albeit rough, quantification, of the printability. Nevertheless, the fabrication of tissue structures is likely to require a significantly higher resolution than what could be evaluated in this approach. In view of this, the visualization of the difference between a computer design and a μCT generated image of a tissue construct, as represented in a heat map,[44] is a promising development, despite the fact that this will not discriminate between different hydrogels in a single generated tissue blueprint.

3. Hydrogel Based Biofabrication Systems

The use of hydrogels as a carrier for cells and/or bioactive compounds has been described for many deposition-based biofabrication approaches.[15, 37] Briefly, these can be divided in methods based on laser-induced forward transfer, inkjet printing (both thermal and piezoelectric) and robotic dispensing (**Fig. 2**). Each technique demanding very specific requirements for characteristics of the hydrogel-based bioinks, with regards to their rheology and post-curing rate in order to achieve reliable fabrication of 3D constructs.

3.1. Laser-Induced Forward Transfer

Laser-induced forward transfer technology refers to the use of a donor slide covered with a laser energy absorbing layer and a layer of cell-containing bioink.[45] The focused laser pulses cause local evaporation of the absorbing layer that, in turn, generates a high gas pressure propelling the bioink compound towards the collector slide (Fig. 2). This technology allows for the precise deposition of materials and (high densities of) cells in relatively small 3D structures without negatively affecting viability or cellular function.[45, 46] It is a nozzle-free approach and is therefore not affected by clogging issues. It has successfully been used with bioinks with a wide range of viscosities (1-300 mPa/s). Nevertheless, the high resolution of this process complicates even distribution of cells over the ejected drops, requires rapid gelation kinetics to achieve high shape fidelity and does result in a relatively low overall flow rate (Fig. 2). Consequently, the generation of larger and thus clinically relevant 3D constructs is time-consuming, hampering the successful translation towards widespread application.

3.2. Inkjet Printing

Usually, inkjet printing in the biofabrication field is defined as the dispensing through a small orifice and precise positioning of very small volumes (1-100 picolitres) of bioink (PBS, cell culture media and/or hydrogel) on a substrate.[2] For the inkjet printing of cells thermal and piezo-electric inkjet printing are the two most commonly adopted approaches. For thermal

inkjet printing (Fig. 2), small volumes of the printing fluid are vaporized by a micro-heater to create the pulse that expels droplets from the print head.[47] The generated heat and resulting evaporation do result in stress for the deposited cells[36] and causes transient pores in the cell membrane.[48] In piezoelectric inkjet printing (Fig. 2), on the other hand, no heating is used, but a direct mechanical pulse is applied to the fluid in the nozzle by a piezoelectric actuator, which causes a shock wave that forces the bioink through the nozzle.

Inkjet printing has successfully been applied for accurate deposition of cells[49] and even allows for the generation of, albeit small, 3D structures.[50] One of the main restrictions of the inkjet technology is perhaps the low upper limit of the viscosity for the ink (Table 1), which is in the order of 0.1 Pa/s,[51] complicating the deposition of higher viscous natural extracellular matrix materials.[52] As small droplets of this ink are deposited onto a substrate with high velocity, the low viscosity will facilitate spreading of the droplet on the surface upon impact. This impedes building up 3D constructs, for which inkjet technology originally was not developed. Moreover, most researchers in this area have been using commercially available inkjet printers, which are designed for dispensing low-viscous inks -not containing particles measuring over 1 μm- at high resolution. Since this involves channels and orifices measuring not much larger than the diameter of a cell, challenges regarding both cell viability and inkjet system reliability result.[53] In summary, as a consequence of the small droplet size and the diffusion-dependent gelation of inkjet printers results in a challenge to translate this technology to larger, more clinically relevant, sizes.

3.3. Robotic Dispensing

An alternative approach for the design and fabrication of organized 3D hydrogel constructs is based on dispensing systems. For this method, hydrogels with suspended cells are generally inserted in disposable plastic syringes and dispensed, either pneumatic, piston- or screw-driven, on a building platform (Fig. 2). Rather than single droplets, robotic dispensing yields

larger hydrogel strands. In order to maintain the shape of the constructs after printing, hydrogels with higher viscosities are often used. Resolution that can be achieved with robotic dispensing is in the order of 200 mm, which is considerably lower compared to laser- or inkjet-based systems. Nevertheless, fabrication speed using robotic dispensing is consequently significantly higher (Table 1) and anatomically shaped constructs have successfully been generated (**Fig. 3**). Piston-driven deposition generally provides more direct control over the flow of the hydrogel from the nozzle, due to the delay of the compressed gas volume in the pneumatic systems. On the other hand, screw-based systems may give more spatial control and are beneficial for the dispensing of hydrogels with higher viscosities. To further improve the printing quality of the 3D constructs, deposition within high viscous crosslinking solutions has been explored.[54, 55] Cells have been deposited with high viability and no notable effects on differentiation capacity using both pneumatic and piston driven systems (see Table 2). Screw extrusion can generate larger pressure drops at the nozzle, which can potentially be harmful for embedded cells. Thus, the screw design needs to be specifically designed to accommodate biofabrication, rather then using off-the-shelf screws designed for other applications. Taken together, robotic dispensing allows the fabrication of organized constructs of clinically-relevant sizes within a realistic time frame, hence this technology is often regarded as the most promising.[37, 38]

4. Key Hydrogel Properties in Biofabrication

The suitability of a hydrogel for a specific biofabrication process mainly depends on its physicochemical properties under the conditions imparted by the specific biofabrication instrument. The development of robust hydrogel systems for biofabrication, *i.e.*, hydrogels that are suitable for both fabrication and cell culture, remains a challenge (Fig. 1). The major physiochemical parameters that determine the printability of a hydrogel are its rheological properties and crosslinking mechanisms **(Fig. 4)**. However, the specific processing parameters, such as nozzle gauge (Fig. 4), will consequently determine the shear stress the embedded cells

are exposed to, as well as the maximal time required for fabrication of a clinically relevant size (cm^3-scale) construct (Fig. 4). Finally, once the hydrogel precursors have been printed and the cells have survived, the printed construct has to possess, develop or be endowed with shape fidelity and sufficient mechanical stability, for example by (post-processing) gelation as a result of crosslinking.

These parameters are interlinked and important for the different biofabrication technologies, however, absolute numbers can be considerably different given the nature of the deposition process. For example, inkjet printing is generally limited to low maximum viscosities, while with robotic dispensing bioinks with higher viscosities can be processed. Accordingly, inkjet printing requires rapid gelation to allow fabrication of an intricate 3D structure. On the other hand, robotic dispensing will facilitate the maintenance of the initial shape after deposition of hihj viscous liquids allowing for gelation (crosslinking) of the generated structures post-fabrication, as well as building large constructs in the x, y, z directions. This illustrates how the viscosity of the hydrogel forming solution dictates how quickly it needs to solidify. In addition, swelling or contraction characteristics of hydrogels must also be considered and taken in account when designing a biofabricated tissue construct of particular size. Moreover, care should be taken when applying different bioinks with dissimilar swelling behaviour, since this can be complicated due to limited grafting of the layers and deformation of the final construct.

4.1. Rheology

Rheology is the study of the flow of matter under application of an external force, and is therefore highly relevant to biofabrication. Nevertheless, its importance is underestimated, given the high number of investigations that do not take rheology into account when developing or evaluating hydrogels for biofabrication. In the instances that rheological data is

presented, it often lacks the clear correlation to the results of the deposition processes, underscoring the complexity of field of rheology and its poorly understood role in biofabrication. Here, we discuss the influence of number of rheological parameters on the biofabrication process.

4.1.1 Viscosity

Viscosity is the resistance of a fluid to flow upon application of a stress. In biofabrication, a high viscosity impedes both surface tension-driven droplet formation (particularly important for filament-based deposition techniques) and the collapse of deposited structures. The viscosity of a polymer solution, such as a hydrogel precursor, is predominantly determined by the polymer concentration and molecular weight. This is illustrated in **Table 3** for a number of hydrogel forming polymers, including sodium alginate (typical molecular weight 200 kDa) and Lutrol F127 (molecular weight 12 kDa). As hydrogels of high polymer concentrations can be restrictive environments for cell proliferation, migration and tissue formation,[56] it seems logical to opt for low concentrations of high molecular weight polymers. This (besides the before mentioned inherent biofunctionality) may explain the popularity and success of naturally derived polymers in the field, as many have high molecular weights that have not been matched by the same extend by synthetic biodegradable alternatives so far. Viscosity of the bioink directly influences shape fidelity after deposition (**Fig. 5**). Low-viscous 20% gelatin methacrylamide (gelMA) solution forms droplets at the needle tip, resulting in the deposition of strands that spread out on the surface, while the increase in viscosity by orders of magnitude upon addition of 2.4% high molecular weight hyaluronic acid (HA), allows the formation of a filament rather than a droplet.[57] Consequently, high-fidelity 3D structures could be deposited in which horizontal pores exist in addition to the vertical pores.

Printing fidelity, thus, generally increases with increasing viscosity, and this is the major underlying reason why hydrogels are usually printed with lower accuracies and resolutions than thermoplastic polymers. However, an increase in viscosity implies an increase of the applied shear stress, which may be harmful for the suspended cells.[58] A plethora of long-term studies on the influence of intermediate shear stress levels on cell attachment and behavior has been performed (e.g., [59] on endothelial cells). For example, at levels in the order of 1Pa endothelial cells may detach from a surface[60] and the morphology and metabolic activity of articular chondrocytes is significantly changed.[61] Much less is known about short-term exposure to very high shear stresses that may arise in printing nozzles and orifices, but cells appear quite resilient in this respect[62] as the viability of printed endothelial cells have been shown to not decrease for shear stress levels up to 1150 kPa,[39] which is 6 orders of magnitude higher than typical values for detaching cells from a surface or influencing cell morphology and metabolism. Within the range of systems, hydrogels and cells used so far, cell viability was generally not severely affected although a (negative) influence of shear stress (higher speeds and thinner nozzles) has been observed for robotic dispensing based systems.[63] In inkjet printing, transient pores have been observed in the cell membrane of printed Chinese hamster ovary cells.[48] These pores, measuring approximately 10 nm, did not negatively affect viability or apoptosis and were self-repaired within 2 hours. Their presence was even used to the benefit of allowing gene transfer through the pores. Besides viscosity, the geometry of the dispensing setup (dimensions of channels, nozzles and/or orifices) and flow rates are additional factors that influence shear stress. In other words, shear stresses may be reduced at the cost of loss of resolution (larger nozzles/orifices) or at the cost of flow rate.

In addition to polymer concentration and molecular weight (as main contributors), viscosity further depends on the solubility parameter (influencing the polymer coil's hydrodynamic

radius), shear rate, temperature and other specific interactions. This means more sophisticated adaptations, which are more likely to ensure proper cellular behavior, are available for improving the rheological behavior of hydrogels for biofabrication.

4.1.2 Shear Thinning

Shear thinning (also pseudo-plasticity) refers to the non-Newtonian behavior in which the viscosity decreases as shear rate increases.[64] It is caused by shear-induced reorganization of the polymer chains to a more stretched conformation, which leads to decreased entanglement and, therefore, viscosity. This phenomenon is, to a variable extent, exhibited by most polymeric systems. Particularly, shear thinning is observed for solution of polymers with high molecular weight. Sodium alginate is an example of a polymer that shows strong shear thinning behavior (**Fig. 6**).[65] At shear rates relevant for 3DF of hydrogels (100-500 s^{-1}), the viscosity is approximately an order of magnitude lower than the plateau value at low shear rates. For higher concentrations, the relative reduction in viscosity induced by shear is even greater. This implies a decreased shear stress at the high shear rates that are present inside a nozzle or orifice during biofabrication, followed by a sharp increase in viscosity (resulting in a high printing fidelity) upon deposition (**Fig. 7**).

4.1.3 Yield Stress

Yield stress is a stress that that must be overcome to initiate flow. Generally interactions between polymer chains result in the formation of a fragile, physically crosslinked network, which is broken by shear forces (above the yield stress) and (slowly) reforms when the shear is removed. Where high viscosity only delays collapse of a deposited 3D structure, the presence of a yield stress can potentially prevent flow and collapse. For example, gellan gum is an anionic polysaccharide that can be crosslinked by cations to form physical networks.[66] When added to gelMA at tailored salt concentrations it forms a gel suitable for robotic

dispensing as it exhibits strong yield stress behavior (Fig. 7).[67] Besides improving printing fidelity, the presence of a yield stress also prevents cell settling in the hydrogel precursor reservoir. Other hydrogel systems that exhibit yield stress and shear-thinning have been developed more specifically for delivering cells or bioactive molecules into the body by injection from a syringe.[64] Among these systems are self-assembling peptide based hydrogels[68], recombinant protein hydrogels[69], colloidal systems[70], gels based on cyclodextrin inclusion complexes and block copolymers.[71]

4.2. Crosslinking mechanisms for hydrogels

Gelation of a printed hydrogel structure is necessary to preserve its shape; even structures constructed from the most viscous precursor solution will change shape due to shape and collapse at some point. The gelation can either be physical (based on reversible interaction), chemical (based on formation of covalent chemical bonds), or a subsequent cascade and combination of both processes (**Fig. 8**).

4.2.1 Physical Crosslinking

Physical crosslinking mechanisms rely on non-chemical interactions based on entanglements of high molecular polymer chains, ionic interactions, hydrogen bridges or hydrophobic interactions. Physically crosslinked hydrogels are the most prominent hydrogel class used for biofabrication processes. For example, the first robotic dispensing approach, as described by Landers et al.,[72] involved printing a physically crosslinked hydrogel into a liquid. Due to the buoyancy of the hydrogels in the liquid, printed constructs are supported, facilitating the generation of porosity in the x-, y-, and z-directions. Gelation is predominantly based on ionic-crosslinking or on a thermally-induced property change and it has been demonstrated that printing into a liquids can also be combined with chemical crosslinking.[73] This strategy

is still being applied, for example by the printing of hydrogels into perfluorinated hydrocarbon-liquids.[54]

One reason for the popularity of physically crosslinked gels is that they have excellent compatibillity with fragile molecules (*e.g.* growth factors) and with living cells, because potentially harmful chemical crosslinking agents are avoided. With physically crosslinked hydrogels, as the name implies, non-covalent physical interactions between hydrophilic polymer chains exist that prevent the gel from (immediate) dissolution in an aqueous environment. Many physical interactions have been exploited to design such physically crosslinked hydrogels, these interactions include hydrogen bonding, ionic interactions (polyelectrolyte hydrogels), stereocomplex formation of polymers or polymer fragments of opposite chirality, and hydrophobic interactions (*e.g.* self-assembly peptides).[74, 75]

4.2.1.1 Ionic Crosslinking

Ionic crosslinking is therefore an important mechanism in biofabrication, particularly for biopolymers. For example, alginate is a polysaccharide that consists of mannuronic and glucuronic acid residues and that is highly soluble in water as Na-salt. However, upon addition of Ca^{2+} ions (or other di/trivalent cations) rapid gelation of alginate occurs. Since this crosslinking occurs under mild and physiological conditions, alginate gels have been studied as system for the controlled release of pharmaceutical proteins and for the entrapment of living cells for TE applications.[76] As a consequence alginate has been widely applied in biofabrication approaches (Table 2). In recent years, hydrogels have also been developed exploiting electrostatic interactions between particles (nano and or micro) of opposite charge dispersed in an aqueous systems. These gels are rapidly formed upon mixing of the particles of opposite charge, but become fluid above a certain shear stress, sufficient to break the

interactions between the charged particles, making them suitable as injectable drug delivery system and likely also for bioprinting.[77]

4.2.1.2 Stereocomplex Crosslinking

Stereocomplex formation occurs, for example, between poly(D-lactic acid) (PDLA) and poly(L-lactic acid) (PLLA), homopolymers of D- and L-lactic acid, respectively. When oligomers of D- and L-lactic acid are coupled to water-soluble polymers like dextran or polyethylene glycol, hydrogels are formed which are crosslinked by stereocomplexes composed of oligomers of opposite chirality. Stereocomplexation does not occur immediately upon mixing of the hydrogel building blocks, allowing their use as injectable systems for controlled drug/protein release and as scaffolds for entrapment of cells.[78] An additional form of complexation mechanisms is the formation of inclusion complexes. For example, cyclodextrins, cyclic oligosaccharides composed of R-1,4-coupled D-glucose units contain a hydrophobic internal cavity that can accommodate lipophilic guest molecules. Cyclodextrins have therefore been investigated for the solubilization of hydrophobic drugs, but also used for the design of super-molecular materials, including hydrogels. In this approach, hydrophilic polymers are derivatized with cyclodextrin units, which, upon mixing with a guest molecule-derivatized polymer, result in the formation of a hydrogel structure. These systems can be readily loaded with bioactive proteins and used as injectable sustained release system.[79]

4.2.1.3 Thermal Crosslinking

Mechanisms described above may be exploited for biofabrication in combination with sensitiveness to changes in external stimuli, especially shear force to yield shear-thinning systems.[64, 80] Of particular interest are systems that are liquid at room temperature, allowing their formulation with bioactive molecules and/or cells, but that gel at body temperature after their administration. Such hydrogels comprise of thermosensitive polymers which have a

good aqueous solubility at room temperature but are insoluble at body temperature. A main representative of thermosensitive polymers is poly(N-isopropylacryl amide) (PNIPAm) which is characterized by a cloud point in water of 32 °C. This polymer has been combined in different architectures with a great variety of water-soluble polymers to yield injectable hydrogels.[81] PNIPAm is, however, not biodegradable and therefore in recent years a number of biodegradable thermosensitive polymers have been described, which were subsequently investigated for TE,[24, 57] as well as for pharmaceutical applications.[82]

4.2.2 Chemical Crosslinking

A significant drawback of the physically crosslinked hydrogels is their poor mechanical properties, which may raise stability problems of a printed construct and be associated with difficulties in handling and its overall performance. Therefore, increasing attention has been given to hydrogels that are hold together by weak (reversible) physical interactions that enable good printability, but that can further be stabilized by chemical crosslinking post-processing. Chemical crosslinking, which comprises all methods that lead to hydrogel formation by connection of gel precursors (low molecular weight monomers or polymeric building blocks) through newly formed covalent bonds, may be tuned to provide hydrogels with good handling properties and high mechanical strength. Chemical crosslinking is usually achieved by mixing of two low viscous solutions with gel precursors (*e.g.* monomers and initiator, complementarily reactive gel precursors), which initiates the crosslinking reaction. This results in a constant increase of viscosity until the gel-point is reached and a 3D polymer network develops. A major drawback of this strategy for biofabrication is the need for very stringent control of crosslinking kinetics from low viscosity printable precursor solutions to the crosslinked hydrogels without blocking the nozzle during the continuous printing process. Yet, shape fidelity of the printed construct has to be guaranteed. One possibility to exploit chemical crosslinking for biofabrication is the use of reactive mixing heads (Fig. 8).

Importantly, these technologies should be developed in such a way that the crosslinking can be done under mild/physiological conditions using chemistry compatible with bioactive proteins and living cells. Hence, chemical crosslinking methods have to be designed in such a way that toxic reaction by products or non-cytocompatible monomers and hydrogel precursors are avoided.

In order to increase the viscosity of the bioprinted gel, hydrogels have also been partially pre-crosslinked prior to deposition.[83] As in the crosslinking process covalent bonds are formed and beyond the gel point the shape is irreversibly fixed, it will be particularly challenging to achieve the desired degree of crosslinking when employing this strategy. Others have ensured high viscosities and fast gelation by initiation of the crosslinking prior to the printing.[84] The continuous development of rheological properties over time during the printing process will likely affect the final shape fidelity. Consequently, chemical crosslinking is mainly used for post-processing fixation and stabilization of printed structures. This approach includes post-stabilizing freshly printed hydrogel constructs, usually weakly stabilized through physical crosslinks, by exposure to radiation, temperature, or by post-processing reaction of complementary chemical groups (*e.g.* by Michael addition reaction[85], click chemistry[86] or enzymatic reactions[87]). Thus, often a cascade of gelation mechanisms and triggers are involved in such systems. For example, the printing of warm gelMA-based solutions that form physical gels upon cooling on the collector, is followed by UV-curing to obtain an irreversibly crosslinked gel.[57] This post-processing photo-polymerization step can lead to very fast crosslinking of the hydrogel and, hence, facilitates the maintenance of shape directly after dispensing.[24, 88] However, UV light has potentially deleterious effects on the embedded cells, and hence its use in biofabrication must take this into account.

5. Converging Biofabrication Strategies

For the fabrication of customized tissue equivalents in tissue engineering, complex anatomical architectures with a certain degree of stiffness may need to be fabricated. Convergence of biofabrication approaches allows for the production of more complex architectures that include overhangs and internal porosity by using sacrificial materials as temporal support during fabrication. Moreover, reinforcing the hydrogel constructs with thermoplastic polymers provides strength, allowing these implants to withstand the mechanical forces they are potentially exposed to within the musculoskeletal system.

5.1. Sacrificial Materials

The CAM-models of complex anatomical structures could easily be derived from a 3D-scan of the part of interest of the human body.[1] Such models often involve overhang geometries due to internal cavities, or due to the outer contour of complex anatomical structures. Through smart rotation of the 3D design, the number of overhangs can be minimized for the AM process. Nevertheless, the remaining overhang geometries need to be temporarily supported, as the deposition of material above an empty cavity will be difficult. Preferably, the temporary support material can be washed away from the target structure serving as a sacrificial component.[89, 90] Sacrificial materials have been implemented in molding processes for creating microchannels in chips.[89, 91] Since these chips were fabricated from inorganic materials the sacrificial components could be removed with a broad spectrum of chemical substances. However, when support materials are a component of viable hydrogel constructs the sacrificial procedure should be cytocompatible. Therefore, sacrificial materials have been applied for realizing channel networks within hydrogel constructs, either by casting[92] or by combining printing and casting.[74, 90] In the latter approach, Miller *et al*.[90] printed a vascular network from carbohydrate glass, a solution of sucrose, glucose and dextran. Subsequently, a hydrogel was cast and crosslinked around this network and the construct was placed in culture medium allowing the printed carbohydrate glass to dissolve. Although this approach provides

exceptional control over the shape of the internal vascular network, with such casting control over the architecture of the surrounding hydrogel construct remains limited. In order to control deposition of different cell types or bioactive substances, the sacrificial material could be applied in a bottom-up AM approach. However, this limits the number of suitable biomaterials. For example, a wide range of water-soluble materials, including carbohydrate glass[90] and polyvinyl alcohol (PVA) are stiff enough to carry their own weight, but form unstable interfaces with the surrounding hydrogel target structures due to their hygroscopic properties. Alternatively, a thermoplastic polymer (e.g. polycaprolactone (PCL)) can be co-deposited as a sacrificial component that forms a stable interface with the hydrogel construct,[93] yet such thermoplastic polymers require physical removal from the target structure, since dissolution using organic solvents would be detrimental the embedded cells. As such, the printed thermoplastic structure serves as a mold and only supports the outer contours.[94] Co-deposition of two stable hydrogels, on the other hand, allows for temporary support of internal cavities, as is the case for tubular structures.[93, 95] In order to dissolve the sacrificial component the target structure needs to be selectively crosslinked.[93]

5.2. Combination with thermoplastic polymers

Biofabricated hydrogel constructs for implantation usually have a lower stiffness than their target tissue, especially for use in the musculoskeletal system[57, 96] A stiff and coherent hydrogel construct will be required to withstand such challenging environments in the human body. Pre-culturing cells in these constructs can increase stiffness due to specific tissue matrix deposition.[97] Yet, this demands high cell concentrations and a substantial preculturing period. Disregarding the influence of incorporated cells, improving stiffness of the hydrogel itself could be achieved by increasing hydrogel crosslink density. Unfortunately, this compromises formation of new tissue partly due to impaired diffusion coefficients of nutrients and wate products through the hydrogel system.[22, 39, 97, 98]

In order to combine favorable biological and mechanical hydrogel properties, reinforcement of hydrogels has been achieved at different levels. Hydrogels have been reinforced by use of double networks (DN)[99] and interpenetrating polymer networks (IPN),[100] as well as by incorporation of nanoparticles[101], nanotubes[96, 101, 102] or electrospun fibers.[103-105] In these approaches the crosslink density of the hydrogel could remain relatively low allowing for adequate tissue formation. However, most of these approaches will not be compatible with AM processes, since fabrication requires casting or a two-step crosslinking reaction. Therefore, recently multiple-tool biofabrication has been developed in which hydrogel constructs are reinforced by co-deposited thermoplastic polymer fibers.[93, 105-108] Specifically, this has been achieved by combining hydrogel and PCL in robotic dispensing[106-108] and by combining electrospinning techniques with inkjet printing[105] or laser-induced forward transfer printing[109]. In this way, hydrogels can be processed at low polymer concentrations while shape and strength of the overall construct are secured by the thermoplastic polymer network. Moreover, it can be used in order to fabricate more complex shaped tissue constructs[93] and the Young's modulus of the target construct can be tailored by adjusting the thermoplastic polymer network.[106, 108] Electrospinning produces a higher resolution of PCL fibers[105, 109] compared to robotic dispensing, and results in a network that better approaches the structure of natural ECM. However, the current solution electrospinning techniques are not able to control fiber deposition and the small pore size of the resulting random meshes limits cell migration.[110] Recently developed melt electrospinning writing techniques[111] address both these limitations,[112] since fibers can be deposited with high spatial resolution and orientation. Combining this technique with hydrogel deposition approaches will allow for the generation of reinforced hydrogel constructs with high control over the intricate spatial organization, although grafting between fibers and the hydrogel needs to be addressed in order to biofabricate truly integrated constructs. In addition, degradation kinetics of these hybrid structures should be understood and controlled. The hydrogel scaffold acts as a

temporary environment and degrades as the embedded cells secrete proteases and subsequently produce extracellular matrix proteins that defines the new tissue. In contrast, the polymeric reinforcement material should degrade in a significant slower rate, providing strength to the developing construct until the tissue has matured and at least once remodeled.

6. Concluding remarks and Future Perspectives

Current deposition and fabrication technologies allow researchers to design and build structures with increasingly intricate architectures. However, in achieving this, many concessions were made with regards to the biological aspects of the hydrogels. The overall lack of suitable bioinks for the generation of larger 3D constructs that replicate a certain degree of tissue organization is hampering both the progress in the field of biofabrication and its translation towards clinical application. In part, this may be due to the current lack of comprehensive and systematic studies that focus on the characterization of the potential bioinks from a physical and rheological point of view. The fact that these physical and rheological properties of hydrogel precursors will interact with its biological performance, highlights the need for novel (semi-) high throughput screening assays since new or altered materials will have to be re-evaluated.

Maintaining high shape fidelity may compromise the biological competence and the clinical potential of the generated structures, due to the physicochemical demands of the hydrogel and the extensive fabrication times. Optimization of the environmental conditions during biofabrication, *e.g.*, printing into a culture medium, may allow for longer fabrication times without negatively affecting the embedded cell viability. Reproduction of the tissues with minute detail is most likely not required,[46, 113] although, this is a relatively unexplored topic in the field and a deeper understanding is urgently needed to which degree the directed organization will contribute to the ultimate organization of the regenerated tissue. A collection

of deposited cells and matrix within a 3D structure is not yet a functional tissue and following the biofabrication, extracellular matrix deposition and remodeling are important processes to form functional tissue structures that will determine the ultimate success of the generated tissue replacement. It will take time to actually achieve the required reorganization and to realize functional interaction of the neo-tissue. Besides this, it remains also to be determined if this reorganization should fully take place after implantation or that an *in vitro* conditioning period, *e.g.*, in a bioreactor with mechanical loading regimes or ectopically in the human body, should be incorporated in the approach. The inclusion of more rigid thermoplastic polymer fibers within hydrogel constructs, either generated by fiber deposition modeling[106] or electrospinning,[103, 112] may assist in taking some of the initial load-bearing, potentially decreasing the bioreactor culture required.

For polymer chemists and material scientists, it remains a challenge to develop unique bioinks, taking in account the required biological competence, the physical requirements dictated by the biofabrication process, as well as the relative toxicity of crosslinking[114] and photo-initiator initiator[115] agents. Promising developments are the generation of IPNs for biomedical applications, including those based on gelatin methacrylamide and gellan gum methacrylate,[37, 99] which demonstrated to have improved mechanical properties while allowing cellular survival. In addition, double-network (DN) hydrogels[116] are an example of hydrogels that have, despite their high water content (~90 wt%), unsurpassed mechanical strength and toughness and are, therefore, suggested as potential full tissue (cartilage) replacements.[117] However, care should be taken in this instance since compression resistance is lost after repeated compression due to breakage of the primary polymer network. Novel DN hydrogels have recently been developed that show partial healing capacity of the primary network.[118] Incorporation of cells in these hydrogel systems will still remain a challenge due to the limited cytocompatibility of the crosslinking agents, as well as to the two-step synthesis

procedure required to create these IPNs,[37, 119] although incorporation as a reinforcing component of a biofabricated construct can be envisioned.

The range of biomaterials that could be applied as bioinks could be extended through the further development of biofabrication methods that can process hydrogel precursor solutions that rely on the addition of a crosslinking agent. Obviously, processing pre-mixed components is problematic due to the increasing viscosity as a result of the initiation of the crosslinking reaction. To avoid crosslinking within the nozzle it is very important to synchronize feed rate and crosslinking kinetics.

An additional important challenge is the scale-up and speed of bioabrication, in order to manufacture constructs of clinically relevant sizes. Approaches to potentially improve production speed include the further convergence of biofabrication technologies, combining approaches with different scales of resolution (*e.g.,* laser-based and robotic dispensing approaches), as well as high throughput production of smaller organized units[120] that can subsequently be assembled in the laboratory or *in situ* in to larger structures.[46] Still often a trade-off between resolution and speed has to be made. While relatively large constructs can be manufactured with robotic dispensing, scale-up issues should be considered for both laser- and inkjet-based systems.[46] With respect to inkjet printing, if systems were to be redesigned specifically for bioprinting with respect to dimensions, the process may become more reliable and of less impact on cell viability and function. Moreover, higher viscosities may be permitted as larger channels and orifices imply lower pressure drops and shear stresses, thereby widening the range of processable hydrogels and facilitating 3D construction. Even at a tenfold decrease in printing resolution (*e.g.* from 1200 dpi to 120 dpi), the minimum feature size (200 mm) may still be acceptable for many bioprinting applications. Although inkjet printers applied for bioprinting purposes were designed to print in 2D, 3D inkjet printers have

recently become commercially available. 3D inkjet printing works by jetting a photo curable resin in thin layers (typically 28 μm) onto a tray, followed immediately by UV curing to prevent spreading of the droplets. In this way, polymer parts of up to 150 mm in height have been fabricated. These developments clearly illustrate the enormous, yet unexplored, potential of inkjet technology.

Taken together, biofabrication potentially allows for further automation, standardization and control of the generation of not only customized implants but also in vitro disease model which allow high-throughput studies. With the suitable bioinks, supported by advanced biofabrication technologies this will also allow us to perform mechanistic studies e.g. how cells interact with their surrounding matrix and/or cells or toxicity screening and drug testing.

Acknowledgements

We extend our thanks to Dr. Paul Dalton for proof reading the manuscript. The research leading to these results has received funding from the European Community's Seventh Framework Programme (FP7/2007-2013) under grant agreements n°309962 (HydroZONES) and n°272286 (PrintCART). Jetze Visser was supported by a grant from the Dutch government to the Netherlands Institute for Regenerative Medicine (NIRM, grant n°FES0908) , Jos Malda was supported by the Dutch Arthritis Foundation and Dietmar W Hutmacher by the Hans Fischer Senior Fellowship , Institute for Advanced Studies, Technical University Munich.

Received: ((will be filled in by the editorial staff))
Revised: ((will be filled in by the editorial staff))
Published online: ((will be filled in by the editorial staff))

References

[1] F. P. W. Melchels, M. A. N. Domingos, T. J. Klein, J. Malda, P. J. Bartolo, D. W. Hutmacher, *Progress in Polymer Science* **2012**, 37, 1079.

[2] P. Calvert, *Science* **2007**, 318, 208.

[3] V. Mironov, T. Boland, T. Trusk, G. Forgacs, R. R. Markwald, *Trends Biotechnol* **2003**, 21, 157.

[4] F. Guillemot, V. Mironov, M. Nakamura, *Biofabrication* **2010**, 2, 010201.

[5] R. J. Shipley, G. W. Jones, R. J. Dyson, B. G. Sengers, C. L. Bailey, C. J. Catt, C. P. Please, J. Malda, *J Theor Biol* **2009**, 259, 489.

[6] S. Catros, J. C. Fricain, B. Guillotin, B. Pippenger, R. Bareille, M. Remy, E. Lebraud, B. Desbat, J. Amedee, F. Guillemot, *Biofabrication* **2011**, 3, 025001; J. N. Hanson Shepherd, S. T. Parker, R. F. Shepherd, M. U. Gillette, J. A. Lewis, R. G. Nuzzo, *Advanced functional materials* **2011**, 21, 47; M. J. Poellmann, K. L. Barton, S. Mishra, A. J. Johnson, *Macromolecular Bioscience* **2011**, 11, 1164; W. S. Choi, D. Ha, S. Park, T. Kim, *Biomaterials* **2011**, 32, 2500; M. Gruene, M. Pflaum, C. Hess, S. Diamantouros, S. Schlie, A. Deiwick, L. Koch, M. Wilhelmi, S. Jockenhoevel, A. Haverich, B. Chichkov, *Tissue engineering. Part C, Methods* **2011**, 17, 973.

[7] F. Marga, K. Jakab, C. Khatiwala, B. Shepherd, S. Dorfman, B. Hubbard, S. Colbert, F. Gabor, *Biofabrication* **2012**, 4, 022001.

[8] V. Mironov, V. Kasyanov, C. Drake, R. R. Markwald, *Regen Med* **2008**, 3, 93.

[9] W. Lee, J. C. Debasitis, V. K. Lee, J. H. Lee, K. Fischer, K. Edminster, J. K. Park, S. S. Yoo, *Biomaterials* **2009**, 30, 1587.

[10] S. V. Murphy, A. Skardal, A. Atala, *Journal of Biomedical Materials Research Part A* **2013**, 101A, 272.

[11] D. L. Cohen, W. Lo, A. Tsavaris, D. Peng, H. Lipson, L. J. Bonassar, *Tissue Eng Part C Methods* **2011**, 17, 239.

[12] B. Duan, L. A. Hockaday, K. H. Kang, J. T. Butcher, *J Biomed Mater Res A* **2013**, 101, 1255.

[13] X. Cui, K. Breitenkamp, M. G. Finn, M. Lotz, D. D. D'Lima, *Tissue Eng Part A* **2012**, 18, 1304.

[14] T. J. Klein, S. C. Rizzi, J. C. Reichert, N. Georgi, J. Malda, W. Schuurman, R. W. Crawford, D. W. Hutmacher, *Macromol Biosci* **2009**, 9, 1049.

[15] N. E. Fedorovich, J. Alblas, J. R. de Wijn, W. E. Hennink, A. J. Verbout, W. J. Dhert, *Tissue Eng* **2007**, 13, 1905.

[16] R. P. Visconti, V. Kasyanov, C. Gentile, J. Zhang, R. R. Markwald, V. Mironov, *Expert Opin Biol Ther* **2010**, 10, 409.

[17] V. Mironov, R. P. Visconti, V. Kasyanov, G. Forgacs, C. J. Drake, R. R. Markwald, *Biomaterials* **2009**, 30, 2164.

[18] D. J. Borg, R. A. Dawson, D. I. Leavesley, D. W. Hutmacher, Z. Upton, J. Malda, *J Biomed Mater Res A* **2009**, 88, 184.

[19] N. C. Hunt, L. M. Grover, *Biotechnology letters* **2010**, 32, 733.

[20] K. L. Spiller, S. A. Maher, A. M. Lowman, *Tissue engineering. Part B, Reviews* **2011**, 17, 281.

[21] M. Dash, F. Chiellini, R. M. Ottenbrite, E. Chiellini, *Progress in Polymer Science* **2011**, 36, 981.

[22] D. Seliktar, *Science* **2012**, 336, 1124.

[23] P. Levett, F. Melchels, K. Schrobback, D. Hutmacher, J. Malda, T. Klein, *submitted* **2013**.

[24] R. Censi, W. Schuurman, J. Malda, G. di Dato, P. E. Burgisser, W. J. A. Dhert, C. F. van Nostrum, P. di Martino, T. Vermonden, W. E. Hennink, *Advanced Functional Materials* **2011**, 21, 1833.

[25] N. E. Fedorovich, J. R. De Wijn, A. J. Verbout, J. Alblas, W. J. Dhert, *Tissue engineering. Part A* **2008**, 14, 127.

[26] N. E. Fedorovich, I. Swennen, J. Girones, L. Moroni, C. A. van Blitterswijk, E. Schacht, J. Alblas, W. J. Dhert, *Biomacromolecules* **2009**, 10, 1689.

[27] C. M. Smith, A. L. Stone, R. L. Parkhill, R. L. Stewart, M. W. Simpkins, A. M. Kachurin, W. L. Warren, S. K. Williams, *Tissue Eng* **2004**, 10, 1566.

[28] C. A. DeForest, K. S. Anseth, *Annual review of chemical and biomolecular engineering* **2012**, 3, 421.

[29] M. Bongio, J. J. van den Beucken, M. R. Nejadnik, S. C. Leeuwenburgh, L. A. Kinard, F. K. Kasper, A. G. Mikos, J. A. Jansen, *European cells & materials* **2011**, 22, 359.

[30] K. Y. Lee, M. C. Peters, K. W. Anderson, D. J. Mooney, *Nature* **2000**, 408, 998; R. Censi, P. Di Martino, T. Vermonden, W. E. Hennink, *J Controlled Release* **2012**, 161, 680.

[31] U. Hersel, C. Dahmen, H. Kessler, *Biomaterials* **2003**, 24, 4385.

[32] A. M. Kasko, D. Y. Wong, *Future medicinal chemistry* **2010**, 2, 1669.

[33] K. Arcaute, B. K. Mann, R. B. Wicker, *Annals of Biomedical Engineering* **2006**, 34, 1429.

[34] T. Billiet, M. Vandenhaute, J. Schelfhout, S. Van Vlierberghe, P. Dubruel, *Biomaterials* **2012**, 33, 6020.

[35] D. Varghese, M. Deshpande, T. Xu, P. Kesari, S. Ohri, T. Boland, *The Journal of thoracic and cardiovascular surgery* **2005**, 129, 470; K. Jakab, A. Neagu, V. Mironov, G. Forgacs, *Biorheology* **2004**, 41, 371.

[36] M. Nakamura, S. Iwanaga, C. Henmi, K. Arai, Y. Nishiyama, *Biofabrication* **2010**, 2, 014110.

[37] B. Derby, *Science* **2012**, 338, 921.

[38] C. J. Ferris, K. G. Gilmore, G. G. Wallace, M. In Het Panhuis, *Appl Microbiol Biotechnol* **2013**.

[39] S. Khalil, W. Sun, *Journal of Biomechanical Engineering-Transactions of the Asme* **2009**, 131, 111002.

[40] A. Tirella, A. Orsini, G. Vozzi, A. Ahluwalia, *Biofabrication* **2009**, 1, 045002.

[41] P. Fardim, *TAPPI Journal* **2002**, 1.

[42] J. J. Ballyns, D. L. Cohen, E. Malone, S. A. Maher, H. G. Potter, T. Wright, H. Lipson, L. J. Bonassar, *Tissue Eng Part C Methods* **2010**, 16, 693.

[43] A. Butscher, M. Bohner, C. Roth, A. Ernstberger, R. Heuberger, N. Doebelin, P. R. von Rohr, R. Muller, *Acta Biomater* **2012**, 8, 373.

[44] L. A. Hockaday, K. H. Kang, N. W. Colangelo, P. Y. Cheung, B. Duan, E. Malone, J. Wu, L. N. Girardi, L. J. Bonassar, H. Lipson, C. C. Chu, J. T. Butcher, *Biofabrication* **2012**, 4, 035005.

[45] L. Koch, M. Gruene, C. Unger, B. Chichkov, *Curr Pharm Biotechnol* **2012**.

[46] B. Guillotin, F. Guillemot, *Trends Biotechnol* **2011**, 29, 183.

[47] B. Derby, *Journal of Materials Chemistry* **2008**, 18, 5717.

[48] X. Cui, D. Dean, Z. M. Ruggeri, T. Boland, *Biotechnol Bioeng* **2010**, 106, 963.

[49] M. Nakamura, A. Kobayashi, F. Takagi, A. Watanabe, Y. Hiruma, K. Ohuchi, Y. Iwasaki, M. Horie, I. Morita, S. Takatani, *Tissue Eng* **2005**, 11, 1658.

[50] K. Arai, S. Iwanaga, H. Toda, C. Genci, Y. Nishiyama, M. Nakamura, *Biofabrication* **2011**, 3, 034113.

[51] P. Calvert, *Chemistry of Materials* **2001**, 13, 3299.

[52] S. Moon, S. K. Hasan, Y. S. Song, F. Xu, H. O. Keles, F. Manzur, S. Mikkilineni, J. W. Hong, J. Nagatomi, E. Haeggstrom, A. Khademhosseini, U. Demirci, *Tissue Eng Part C Methods* **2010**, 16, 157.

[53] D. Chahal, A. Ahmadi, K. C. Cheung, *Biotechnol Bioeng* **2012**, 109, 2932.

[54] D. F. Duarte Campos, A. Blaeser, M. Weber, J. Jakel, S. Neuss, W. Jahnen-Dechent, H. Fischer, *Biofabrication* **2013**, 5, 015003.

[55] P. S. Maher, R. P. Keatch, K. Donnelly, R. E. Mackay, J. Z. Paxton, *Rapid Prototyping Journal* **2009**, 15, 204.

[56] S. J. Bryant, K. S. Anseth, *Journal of Biomedical Materials Research* **2002**, 59, 63; G. D. Nicodemus, S. J. Bryant, *Tissue Engineering Part B-Reviews* **2008**, 14, 149.

[57] W. Schuurman, P. A. Levett, M. W. Pot, P. R. van Weeren, W. J. Dhert, D. W. Hutmacher, F. P. Melchels, T. J. Klein, J. Malda, *Macromol Biosci* **2013**, doi: 10.1002/mabi.201200471.

[58] B. A. Aguado, W. Mulyasasmita, J. Su, K. J. Lampe, S. C. Heilshorn, *Tissue Eng Part A* **2012**, 18, 806.

[59] P. Feugier, R. A. Black, J. A. Hunt, T. V. How, *Biomaterials* **2005**, 26, 1457; M. Morigi, C. Zoja, M. Figliuzzi, M. Foppolo, G. Micheletti, M. Bontempelli, M. Saronni, G. Remuzzi, A. Remuzzi, *Blood* **1995**, 85, 1696; A. D. van der Meer, A. A. Poot, J. Feijen, I. Vermes, *Biomicrofluidics* **2010**, 4.

[60] D. K. Macario, I. Entersz, J. P. Abboud, G. B. Nackman, *J Surg Res* **2008**, 147, 282.

[61] R. L. Smith, D. R. Carter, D. J. Schurman, *Clin Orthop Relat Res* **2004**, S89.

[62] R. E. Saunders, J. E. Gough, B. Derby, *Biomaterials* **2008**, 29, 193.

[63] N. E. Fedorovich, W. Schuurman, H. M. Wijnberg, H. J. Prins, P. R. van Weeren, J. Malda, J. Alblas, W. J. Dhert, *Tissue Eng Part C Methods* **2012**, 18, 33.

[64] M. Guvendiren, H. D. Lu, J. A. Burdick, *Soft Matter* **2012**, 8, 260.

[65] R. A. Rezende, P. J. Bartolo, A. Mendes, R. Maciel, *Journal of Applied Polymer Science* **2009**, 113, 3866.

[66] J. M. Tang, M. A. Tung, Y. Y. Zeng, *Carbohydrate Polymers* **1996**, 29, 11.

[67] F. P. W. Melchels, D. W. Hutmacher, J. Malda, **2013**, in preparation.

[68] R. J. Mart, R. D. Osborne, M. M. Stevens, R. V. Ulijn, *Soft Matter* **2006**, 2, 822.

[69] S. Banta, I. R. Wheeldon, M. Blenner, *Annual Review of Biomedical Engineering, Vol 12* **2010**, 12, 167.

[70] Q. Wang, J. Wang, Q. Lu, M. S. Detamore, C. Berkland, *Biomaterials* **2010**, 31, 4980.

[71] J. Araki, K. Ito, *Soft Matter* **2007**, 3, 1456.

[72] R. Landers, U. Hubner, R. Schmelzeisen, R. Mulhaupt, *Biomaterials* **2002**, 23, 4437.

[73] A. Pfister, R. Landers, A. Laib, U. Hubner, R. Schmelzeisen, R. Mulhaupt, *Journal of Polymer Science: Part A: Polymer Chemistry* **2004**, 42, 624.

[74] C. C. Chang, E. D. Boland, S. K. Williams, J. B. Hoying, *Journal of Biomedical Materials Research Part B-Applied Biomaterials* **2011**, 98B, 160.

[75] P. Y. W. Dankers, M. C. Harmsen, L. A. Brouwer, M. J. A. Van Luyn, E. W. Meijer, *Nature Materials* **2005**, 4, 568.

[76] P. Gacesa, *Carbohydrate Polymers* **1988**, 8, 162; S. Wee, W. R. Gombotz, *Adv Drug Deliv Rev* **1998**, 31, 267; Y. M. Kolambkar, K. M. Dupont, J. D. Boerckel, N. Huebsch, D. J. Mooney, D. W. Hutmacher, R. E. Guldberg, *Biomaterials* **2011**, 32, 65.

[77] S. R. Van Tomme, M. J. van Steenbergen, S. C. De Smedt, C. F. van Nostrum, W. E. Hennink, *Biomaterials* **2005**, 26, 2129; Q. Wang, L. Wang, M. S. Detamore, C. Berkland, *Adv Mater* **2008**, 20, 236.

[78] S. J. de Jong, W. N. E. van Dijk-Wolthuis, J. J. Kettenes-van den Bosch, P. J. W. Schuyl, W. E. Hennink, *Macromolecules* **1998**, 31, 6397; I. Rashkov, N. Manolova, S. M. Li, J. L. Espartero, M. Vert, *Macromolecules* **1996**, 29, 50; S. J. Buwalda, P. J. Dijkstra, L. Calucci, C. Forte, J. Feijen, *Biomacromolecules* **2010**, 11, 224.

[79] L. Li, X. Guo, J. Wang, P. Liu, R. K. Prud'homme, B. L. May, S. F. Lincoln, *Macromolecules* **2008**, 41, 8677; F. van de Manakker, K. Braeckmans, N. el Morabit, S. C. De Smedt, C. F. van Nostrum, W. E. Hennink, *Adv Funct Mater* **2009**, 19, 2992; O.

Kretschmann, S. W. Choi, M. Miyauchi, I. Tomatsu, A. Harada, H. Ritter, *Angewandte Chemie. International Ed.* **2006**, 45, 4361.

[80] W. E. Hennink, C. F. van Nostrum, *Advanced Drug Delivery Reviews* **2002**, 54, 13.

[81] S. Chaterji, I. K. Kwon, K. Park, *Progress in Polymer Science* **2007**, 32, 1083; N. A. Peppas, W. Leobandung, *J Biomater Sci Polym Ed* **2004**, 15, 125; J. D. Thomas, G. Fussell, S. Sarkar, A. M. Lowman, M. Marcolongo, *Acta Biomater* **2010**, 6, 1319.

[82] L. Klouda, A. G. Mikos, *Eur J Pharm Biopharm* **2008**, 68, 34; M. K. Joo, M. H. Park, B. G. Choia, B. Jeong, *J Mat Chem* **2009**, 19, 5891; M. H. Park, M. K. Joo, B. G. Choi, B. Jeong, *Account of Chemical Research* **2012**, 45, 424; T. Vermonden, R. Censi, W. E. Hennink, *Chem Rev* **2012**, 112, 2853.

[83] A. Skardal, J. Zhang, L. McCoard, X. Xu, S. Oottamasathien, G. D. Prestwich, *Tissue Eng Part A* **2010**, 16, 2675.

[84] D. L. Cohen, E. Malone, H. Lipson, L. J. Bonassar, *Tissue Eng* **2006**, 12, 1325.

[85] R. Censi, P. J. Fieten, P. Di Martino, W. E. Hennink, T. Vermonden, *J Control Release* **2010**, 148, e28.

[86] E. Lallana, A. Sousa-Herves, F. Fernandez-Trillo, R. Riguera, E. Fernandez-Megia, *Pharm Res* **2012**, 29, 1.

[87] L. S. Teixeira, J. Feijen, C. A. van Blitterswijk, P. J. Dijkstra, M. Karperien, *Biomaterials* **2012**, 33, 1281.

[88] L. Pescosolido, W. Schuurman, J. Malda, P. Matricardi, F. Alhaique, T. Coviello, P. R. van Weeren, W. J. Dhert, W. E. Hennink, T. Vermonden, *Biomacromolecules* **2011**, 12, 1831.

[89] F. Dang, S. Shinohara, O. Tabata, Y. Yamaoka, M. Kurokawa, Y. Shinohara, M. Ishikawa, Y. Baba, *Lab on a chip* **2005**, 5, 472.

[90] J. S. Miller, K. R. Stevens, M. T. Yang, B. M. Baker, D. H. Nguyen, D. M. Cohen, E. Toro, A. A. Chen, P. A. Galie, X. Yu, R. Chaturvedi, S. N. Bhatia, C. S. Chen, *Nature materials* **2012**, 11, 768.

[91] Z. Gan, L. Zhang, G. Chen, *Electrophoresis* **2011**, 32, 3319; H. A. Reed, C. E. White, V. Rao, S. A. B. Allen, C. L. Henderson, P. A. Kohl, *Journal of Micromechanics and Microengineering* **2001**, 11, 733.

[92] A. P. Golden, J. Tien, *Lab on a chip* **2007**, 7, 720; Y. Ling, J. Rubin, Y. Deng, C. Huang, U. Demirci, J. M. Karp, A. Khademhosseini, *Lab on a chip* **2007**, 7, 756.

[93] J. Visser, B. J. Peters, T. J. Burger, J. Boomstra, W. J. Dhert, F. Melchels, J. Malda, *under review* **2013**.

[94] A. J. Reiffel, C. Kafka, K. A. Hernandez, S. Popa, J. L. Perez, S. Zhou, S. Pramanik, B. N. Brown, W. S. Ryu, L. J. Bonassar, J. A. Spector, *PLoS One* **2013**, 8, e56506.

[95] A. Skardal, J. Zhang, G. D. Prestwich, *Biomaterials* **2010**, 31, 6173.

[96] S. R. Shin, H. Bae, J. M. Cha, J. Y. Mun, Y. C. Chen, H. Tekin, H. Shin, S. Farshchi, M. R. Dokmeci, S. Tang, A. Khademhosseini, *ACS nano* **2012**, 6, 362.

[97] I. E. Erickson, S. R. Kestle, K. H. Zellars, M. J. Farrell, M. Kim, J. A. Burdick, R. L. Mauck, *Acta Biomaterialia* **2012**, 8, 3027.

[98] P. N. Patel, A. S. Gobin, J. L. West, C. W. Patrick, Jr., *Tissue Eng* **2005**, 11, 1498.

[99] H. Shin, B. D. Olsen, A. Khademhosseini, *Biomaterials* **2012**, 33, 3143.

[100] S. Suri, C. E. Schmidt, *Acta Biomaterialia* **2009**, 5, 2385; D. Myung, W. U. Koh, J. M. Ko, Y. Hu, M. Carrasco, J. Noolandi, C. N. Ta, C. W. Frank, *Polymer* **2007**, 48, 5376.

[101] S. Min Kyoon, I. K. Sun, K. Seon Jeong, K. Byung Joo, S. Insuk, E. K. Mikhail, O. Jiyoung, H. B. Ray, *Appl. Phys. Lett.* **2008**, 93, 3.

[102] G.-G. S. Saez-Martinez V, Vera C, Olalde B, Madarieta I, Obieta I, Garagorri N, *Journal of Applied Polymer Science* **2010**, 120, 6.

[103] J. Coburn, M. Gibson, P. A. Bandalini, C. Laird, H. Q. Mao, L. Moroni, D. Seliktar, J. Elisseeff, *Smart Structures and Systems* **2011**, 7, 213.

[104] J. M. Coburn, M. Gibson, S. Monagle, Z. Patterson, J. H. Elisseeff, *Proc Natl Acad Sci U S A* **2012**, 109, 10012.

[105] T. Xu, K. W. Binder, M. Z. Albanna, D. Dice, W. Zhao, J. J. Yoo, A. Atala, *Biofabrication* **2012**, 5, 015001.

[106] W. Schuurman, V. Khristov, M. W. Pot, P. R. van Weeren, W. J. Dhert, J. Malda, *Biofabrication* **2011**, 3, 021001.

[107] J. H. Shim, J. Y. Kim, M. Park, J. Park, D. W. Cho, *Biofabrication* **2011**, 3, 034102.

[108] H. Lee, S. Ahn, L. J. Bonassar, G. Kim, *Macromolecular rapid communications* **2012**.

[109] S. Catros, F. Guillemot, A. Nandakumar, S. Ziane, L. Moroni, P. Habibovic, C. van Blitterswijk, B. Rousseau, O. Chassande, J. Amedee, J. C. Fricain, *Tissue engineering. Part C, Methods* **2012**, 18, 62.

[110] Q. P. Pham, U. Sharma, A. G. Mikos, *Biomacromolecules* **2006**, 7, 2796.

[111] B. L. Farrugia, T. D. Brown, D. W. Hutmacher, Z. Upton, P. D. Dalton, T. R. Dargaville, *Biofabrication* **2013**, 5, 025001; P. D. Dalton, C. Vaquette, B. L. Farrugia, T. R. Dargaville, T. D. Brown, D. W. Hutmacher, *Biomaterials Science* **2013**, Advance Article.

[112] T. D. Brown, P. D. Dalton, D. W. Hutmacher, *Adv Mater* **2011**, 23, 5651.

[113] G. Forgacs, *Nat Mater* **2012**, 11, 746.

[114] J. S. Temenoff, H. Shin, D. E. Conway, P. S. Engel, A. G. Mikos, *Biomacromolecules* **2003**, 4, 1605.

[115] C. G. Williams, A. N. Malik, T. K. Kim, P. N. Manson, J. H. Elisseeff, *Biomaterials* **2005**, 26, 1211.

[116] J. A. Johnson, N. J. Turro, J. T. Koberstein, J. E. Mark, *Progress in Polymer Science* **2010**, 35, 332; M. A. Haque, T. Kurokawa, J. P. Gong, *Polymer* **2012**, 53, 1805.

[117] C. Azuma, K. Yasuda, Y. Tanabe, H. Taniguro, F. Kanaya, A. Nakayama, Y. M. Chen, J. P. Gong, Y. Osada, *J Biomed Mater Res A* **2007**, 81, 373.

[118] K. Harrass, R. Kruger, M. Moller, K. Albrecht, J. Groll, *Soft Matter* **2013**, 9, 2869.

[119] J. P. Gong, *Soft Matter* **2010**, 6, 2583.

[120] N. C. Rivron, J. Rouwkema, R. Truckenmuller, M. Karperien, J. De Boer, C. A. Van Blitterswijk, *Biomaterials* **2009**, 30, 4851.

[121] L. Koch, A. Deiwick, S. Schlie, S. Michael, M. Gruene, V. Coger, D. Zychlinski, A. Schambach, K. Reimers, P. M. Vogt, B. Chichkov, *Biotechnology and bioengineering* **2012**, 109, 1855.

[122] B. Guillotin, A. Souquet, S. Catros, M. Duocastella, B. Pippenger, S. Bellance, R. Bareille, M. Remy, L. Bordenave, J. Amedee, F. Guillemot, *Biomaterials* **2010**, 31, 7250.

[123] J. Yan, Y. Huang, D. B. Chrisey, *Biofabrication* **2013**, 5, 015002.

[124] T. Boland, T. Xu, B. Damon, X. Cui, *Biotechnology journal* **2006**, 1, 910.

[125] T. Xu, W. Zhao, J. M. Zhu, M. Z. Albanna, J. J. Yoo, A. Atala, *Biomaterials* **2013**, 34, 130.

[126] K. Jakab, C. Norotte, B. Damon, F. Marga, A. Neagu, C. L. Besch-Williford, A. Kachurin, K. H. Church, H. Park, V. Mironov, R. Markwald, G. Vunjak-Novakovic, G. Forgacs, *Tissue Engineering Part A* **2008**, 14, 413.

[127] R. Landers, A. Pfister, U. Hubner, H. John, R. Schmelzeisen, R. Mulhaupt, *Journal of Materials Science* **2002**, 37, 3107.

[128] C. Norotte, F. S. Marga, L. E. Niklason, G. Forgacs, *Biomaterials* **2009**, 30, 5910.

[129] D. L. Cohen, J. I. Lipton, L. J. Bonassar, H. Lipson, *Biofabrication* **2010**, 2, 035004.

[130] S. Khalil, J. Nam, W. Sun, *Rapid Prototyping Journal* **2005**, 11, 9.

[131] J. H. Shim, J. S. Lee, J. Y. Kim, D. W. Cho, *Journal of Micromechanics and Microengineering* **2012**, 22, 085014.

[132] S. J. Song, J. Choi, Y. D. Park, S. Hong, J. J. Lee, C. B. Ahn, H. Choi, K. Sun, *Artificial organs* **2011**, 35, 1132.

[133] Y. N. Yan, X. H. Wang, Z. Xiong, H. X. Liu, F. Liu, F. Lin, R. D. Wu, R. J. Zhang, Q. P. Lu, *Journal of Bioactive and Compatible Polymers* **2005**, 20, 259.

[134] C. M. Smith, J. J. Christian, W. L. Warren, S. K. Williams, *Tissue Eng* **2007**, 13, 373.

[135] W. Lee, V. Lee, S. Polio, P. Keegan, J. H. Lee, K. Fischer, J. K. Park, S. S. Yoo, *Biotechnology and bioengineering* **2010**, 105, 1178.

[136] X. Wang, Y. Yan, Y. Pan, Z. Xiong, H. Liu, J. Cheng, F. Liu, F. Lin, R. Wu, R. Zhang, Q. Lu, *Tissue Engineering* **2006**, 12, 83.

[137] T. Zhang, Y. N. Yan, X. H. Wang, Z. Xiong, F. Lin, R. D. Wu, R. J. Zhang, *Journal of Bioactive and Compatible Polymers* **2007**, 22, 19.

[138] S. J. Li, Z. Xiong, X. H. Wang, Y. N. Yan, H. X. Liu, R. J. Zhang, *Journal of Bioactive and Compatible Polymers* **2009**, 24, 249.

[139] M. Xu, X. Wang, Y. Yan, R. Yao, Y. Ge, *Biomaterials* **2010**, 31, 3868.

[140] Y. Yan, X. Wang, Y. Pan, H. Liu, J. Cheng, Z. Xiong, F. Lin, R. Wu, R. Zhang, Q. Lu, *Biomaterials* **2005**, 26, 5864.

[141] J. Cheng, F. Lin, H. X. Liu, Y. N. Yan, X. H. Wang, R. Zhang, Z. Xiong, *Journal of Manufacturing Science and Engineering-Transactions of the Asme* **2008**, 130.

[142] W. Xu, X. H. Wang, Y. N. Yan, W. Zheng, Z. Xiong, F. Lin, R. D. Wu, R. J. Zhang, *Journal of Bioactive and Compatible Polymers* **2007**, 22, 363.

[143] J. E. Snyder, Q. Hamid, C. Wang, R. Chang, K. Emami, H. Wu, W. Sun, *Biofabrication* **2011**, 3, 034112.

[144] K. Iwami, T. Noda, K. Ishida, K. Morishima, M. Nakamura, N. Umeda, *Biofabrication* **2010**, 2, 014108.

[145] P. Gonzaleztello, F. Camacho, G. Blazquez, *Journal of Chemical and Engineering Data* **1994**, 39, 611.

[146] D. M. Knapp, V. H. Barocas, A. G. Moon, K. Yoo, L. R. Petzold, R. T. Tranquillo, *Journal of Rheology* **1997**, 41, 971.

Figures

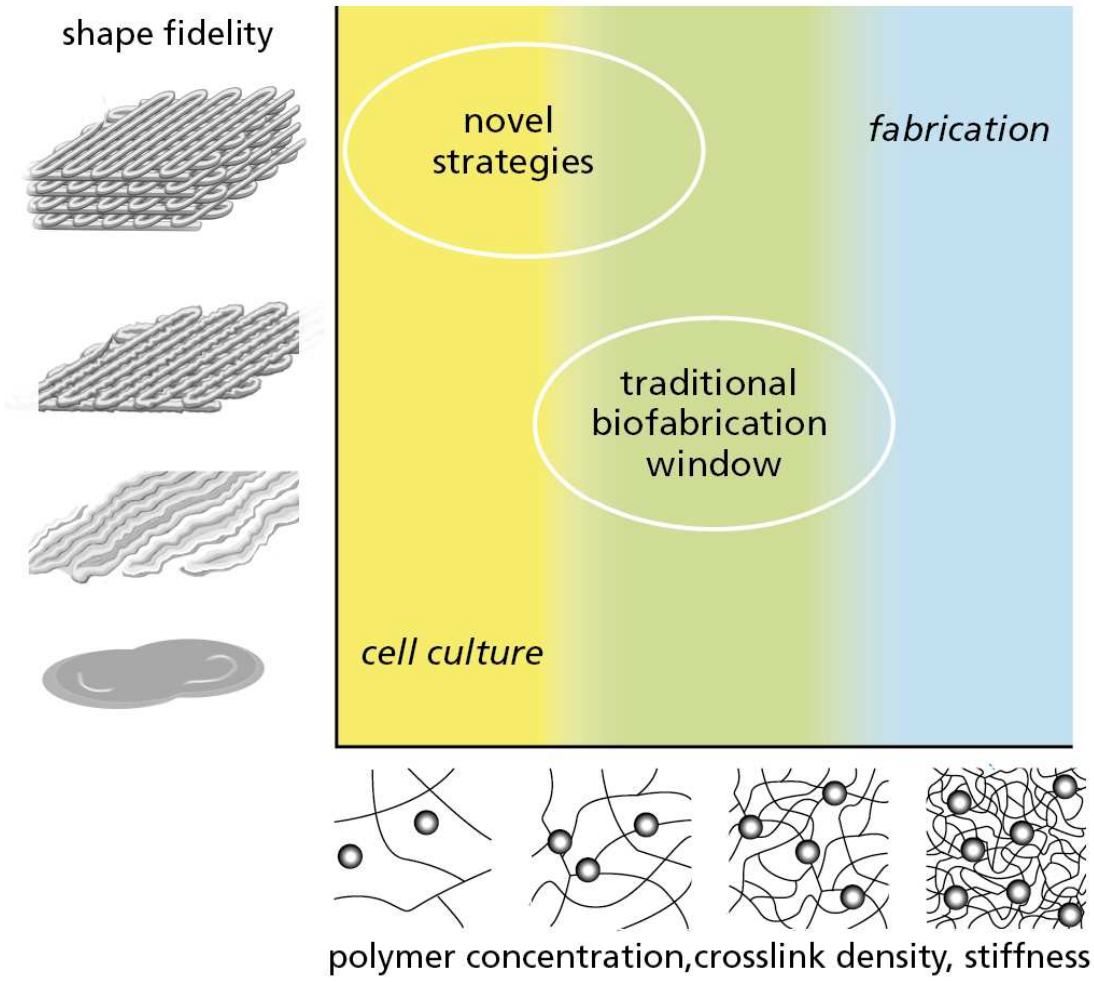

Figure 1. This review advocates a change in the paradigm of biopolymer development by shifting the biofabrication window. Optimal shape fidelity in biofabrication processes can typically be achieved with stiff hydrogels containing high polymer concentrations /or crosslink densities (fabrication window), however, this dense polymer network limits cell migration, growth and differentiation. On the other end of the spectrum, cells thrive best in soft hydrogels (cell culture window), which are to watery too maintain shape for fabrication purposes. Therefore, a biofabrication window exists for medium crosslinked hydrogels,[39] compromising on both biological and fabrication properties. Recently, strategies are applied to shift the bioprinting window, obtaining high shape fidelity with cytocompatible hydrogels.

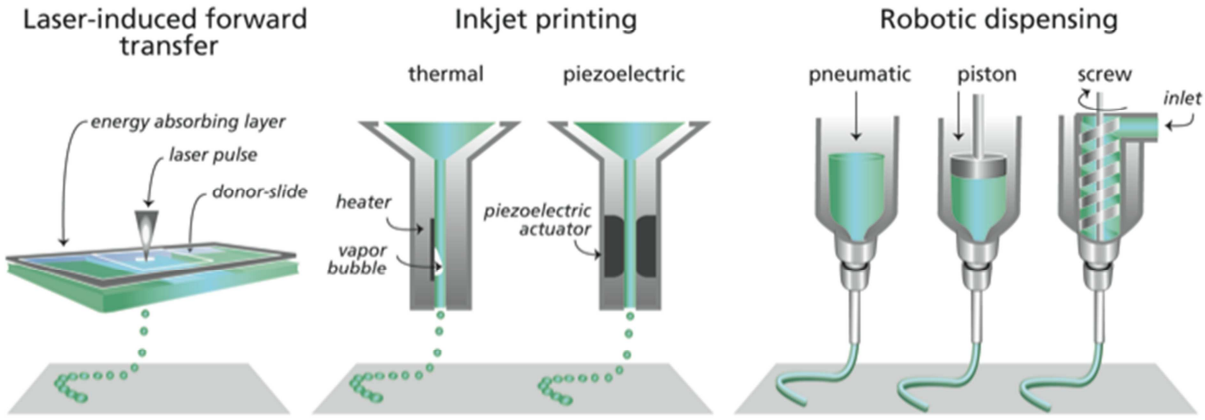

Figure 2. Selected biofabrication approaches involving the use of hydrogels in form of a so called “bioink”.

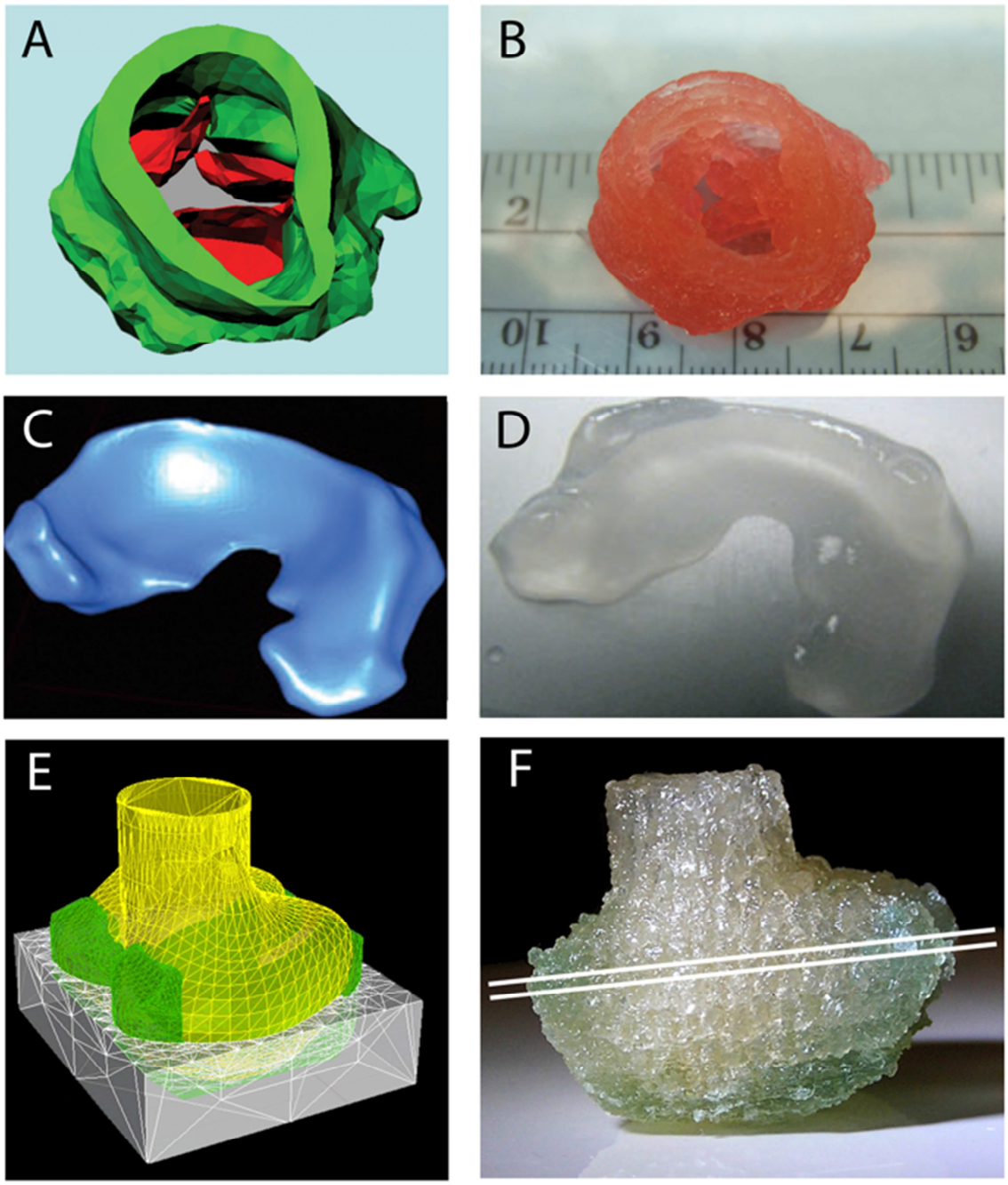

Figure 3. Biofabrication examples - Aortic valve model reconstructed from micro-CT images (A). The root and leaflet regions rendered separately into 3D geometries (green color indicates valve root and red color indicates valve leaflets) and printed (B). An ovine meniscus reconstructed from micro-CT images (C) and printed (D). A miniaturized distal femur from a human knee designed using Rhino Software LxWxH: 40x35x32mm) containing a cartilage layer (green) and a bone component (yellow) and a support structure (white) (E) and printed after manual removal of the support structure (F). Reproduced with permission from Duan *et al.*[12] and Wiley (A,B), Cohen *et al.*[11] Liebert (C,D), and Visser *et al.*[93] (E, F).

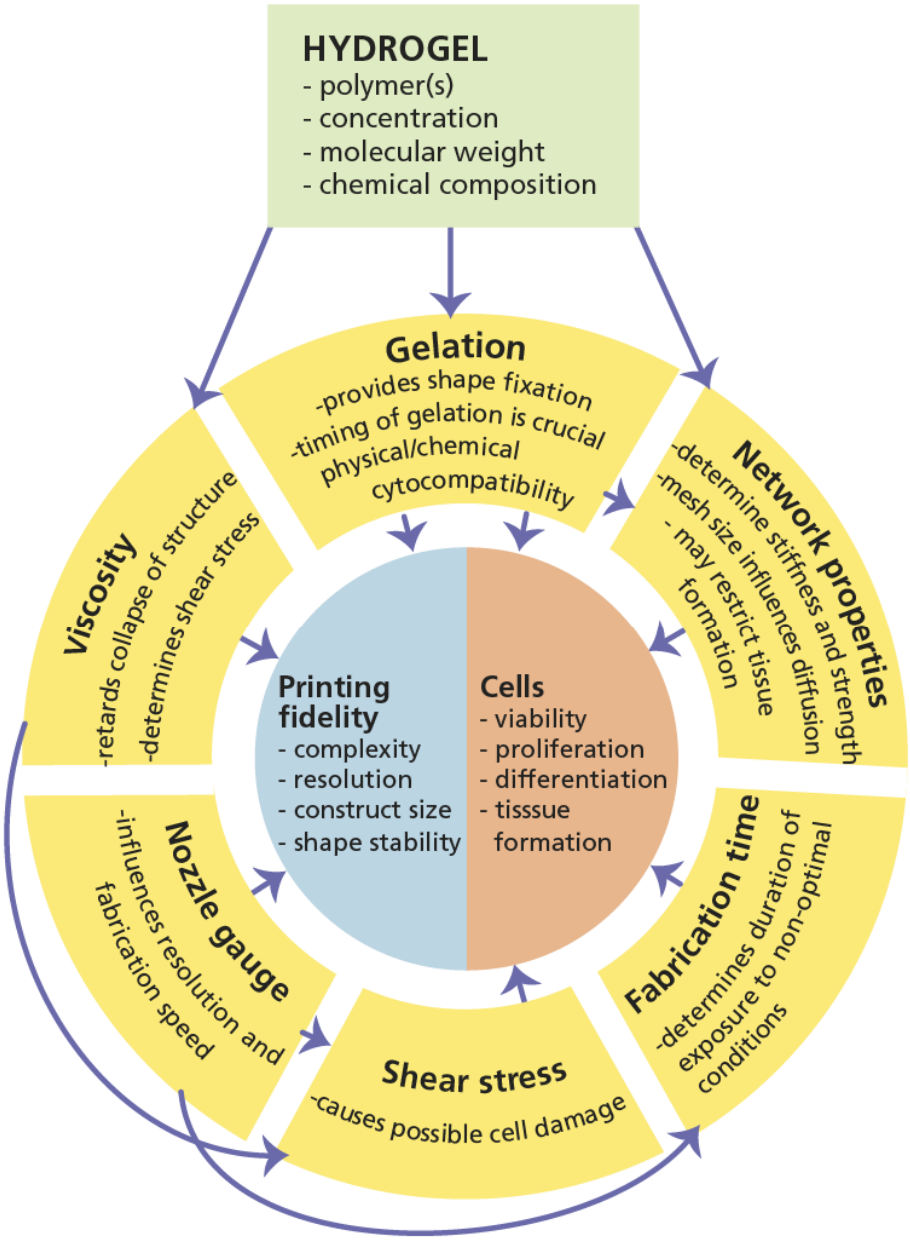

Figure 4. Concept map of variables and relations critical to biofabrication. The hydrogel (polymer type(s), concentration, molecular weight and chemical composition) directly determines the viscosity, gelation mechanism and speed, and mechanical properties of the final gel. This -in combination with processing parameters, such as nozzle gauge and fabrication time- influence the main outcomes *Printing fidelity* and *Cell* viability and function.

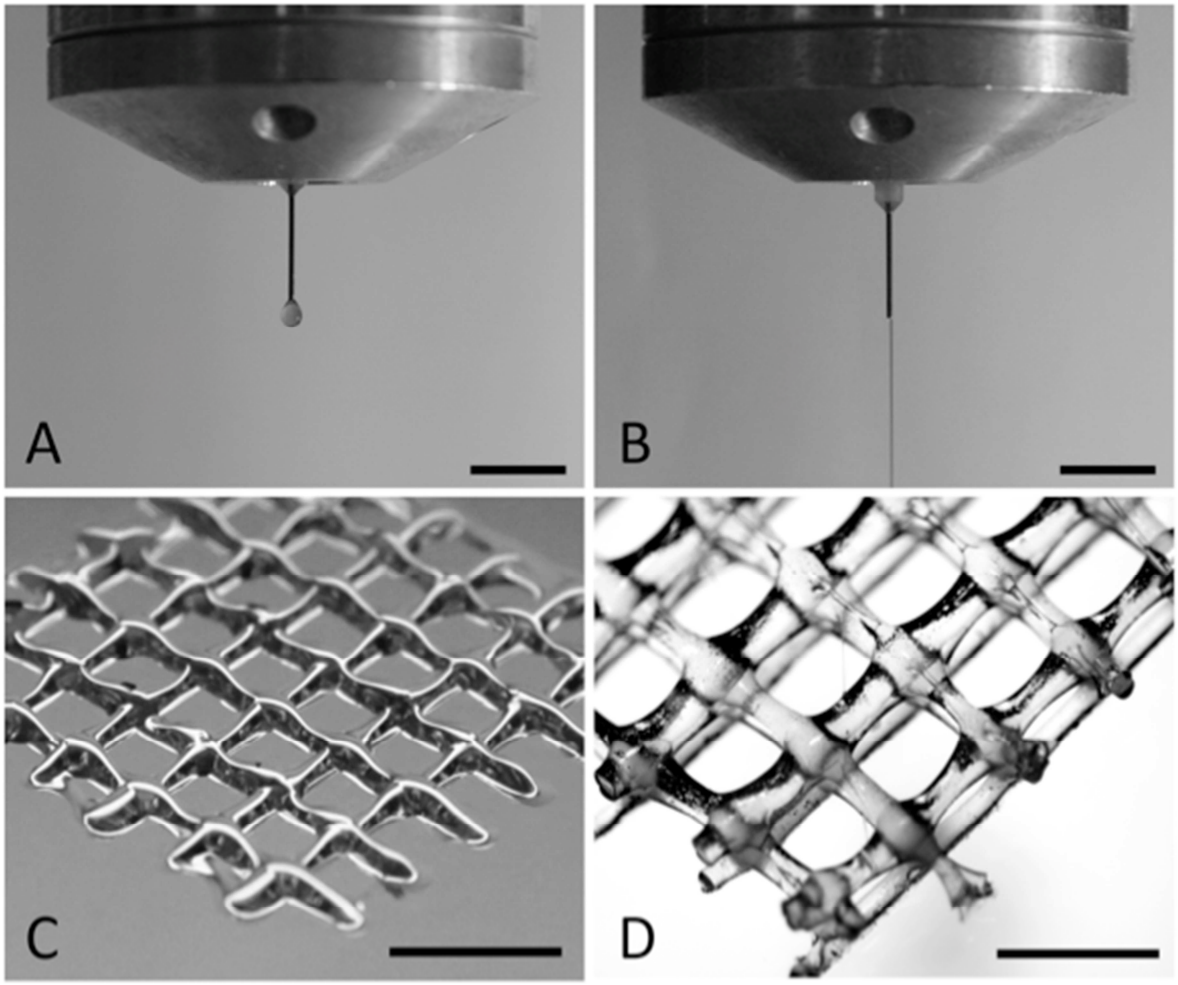

Figure 5. Illustration of the role of viscosity in bioprinting. Gelatin methacrylamide (gelMA) on its own (20%) formes droplets at the nozzle (A) and deposits in flat lines that spread out on the surface (C). When 2.4% hyaluronic acid (HA) is added, strands can be deposited from the nozzle (B), resulting in a construct of four layers (D). The scale bars in A-C represent 5 mm; the scale bar in D is 2 mm. Reproduced with permission from Schuurman *et al*.[57] and Wiley.

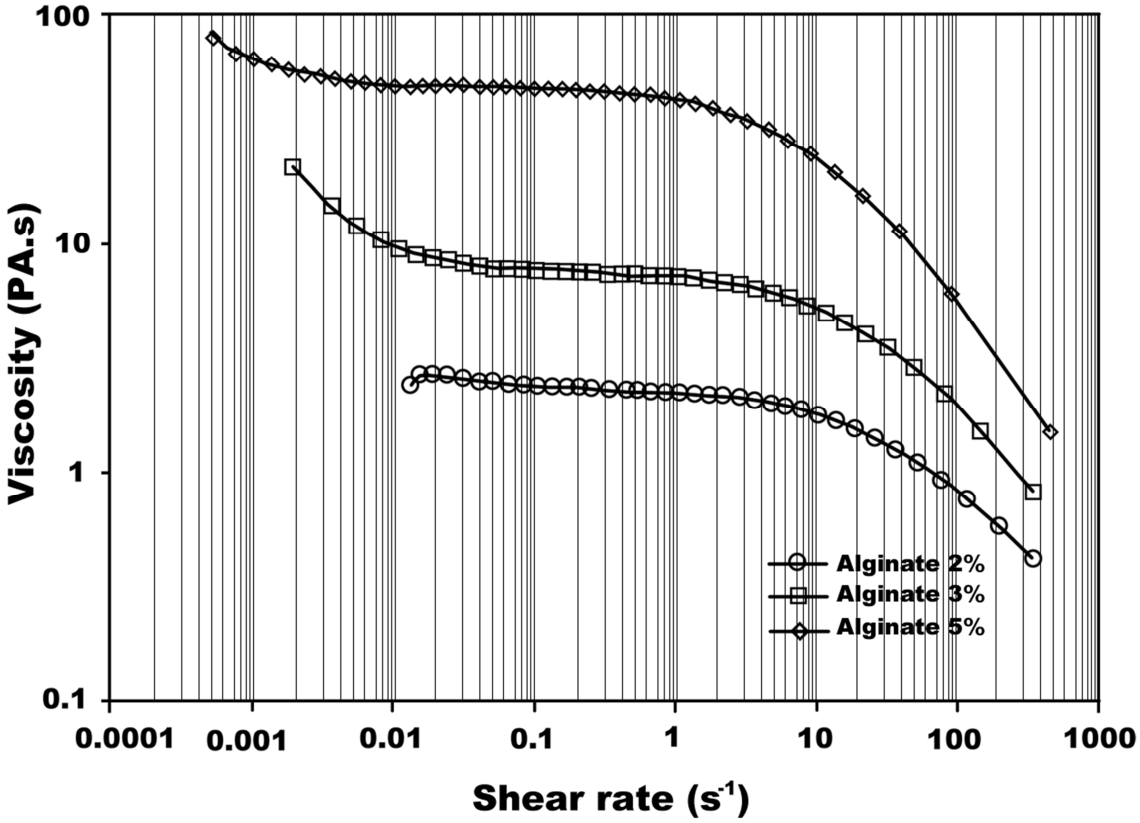

Figure 6. Viscosity variation as a function of shear rate for different alginate solutions. Shear thinning is demonstrated by the rapid decline in viscosity as the shear rate is increased, with higher concentration alginate having the greatest reduction in shear viscosity. Reproduced with permission from Rezende *et al*.[65] and Wiley.

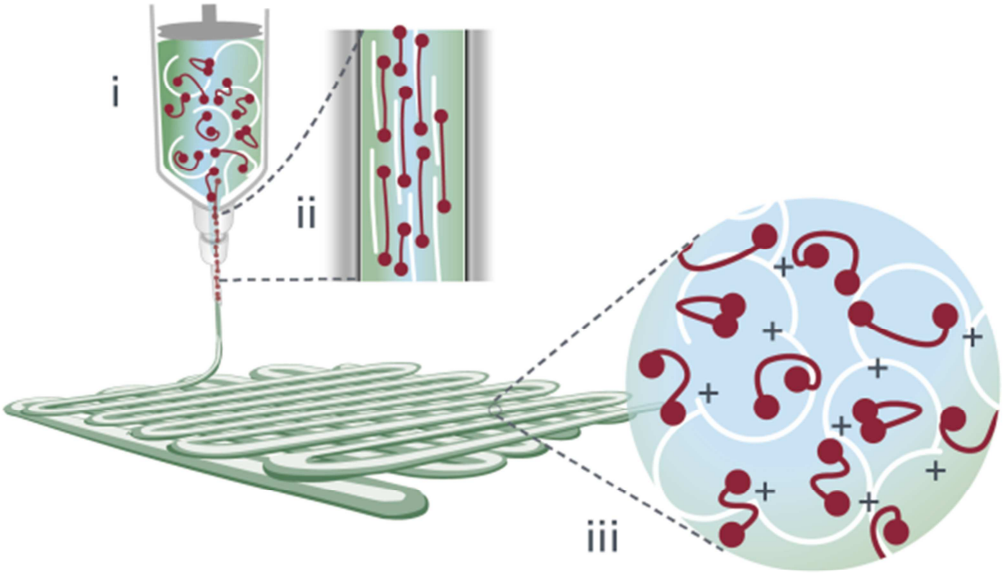

Figure 7. Schematic representation of shear thinning and yield stress in plotting gelatin methacrylamide (gelMA)/gellan gum. In the syringe the gellan chains (in white) form a temporary network and induce gel-like viscosity (i). Upon dispensing through a needle, the temporary network is broken up by shear and all polymer chains align, reducing the viscosity by orders of magnitude (ii). Directly after removal of shear stress, the temporary network is restored and the plotted filament solidifies instantly (iii). Reproduced with permission from Melchels *et al.*[67]

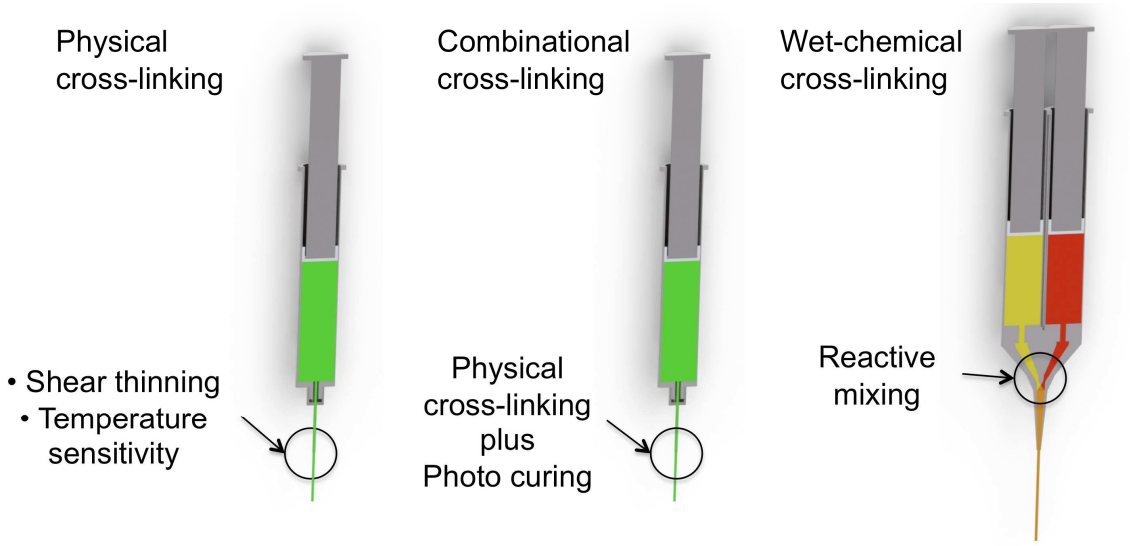

Figure 8. Graphical illustration of physical, combinational and wet-chemical crosslinking mechanisms for extrusion-based biofabrication.

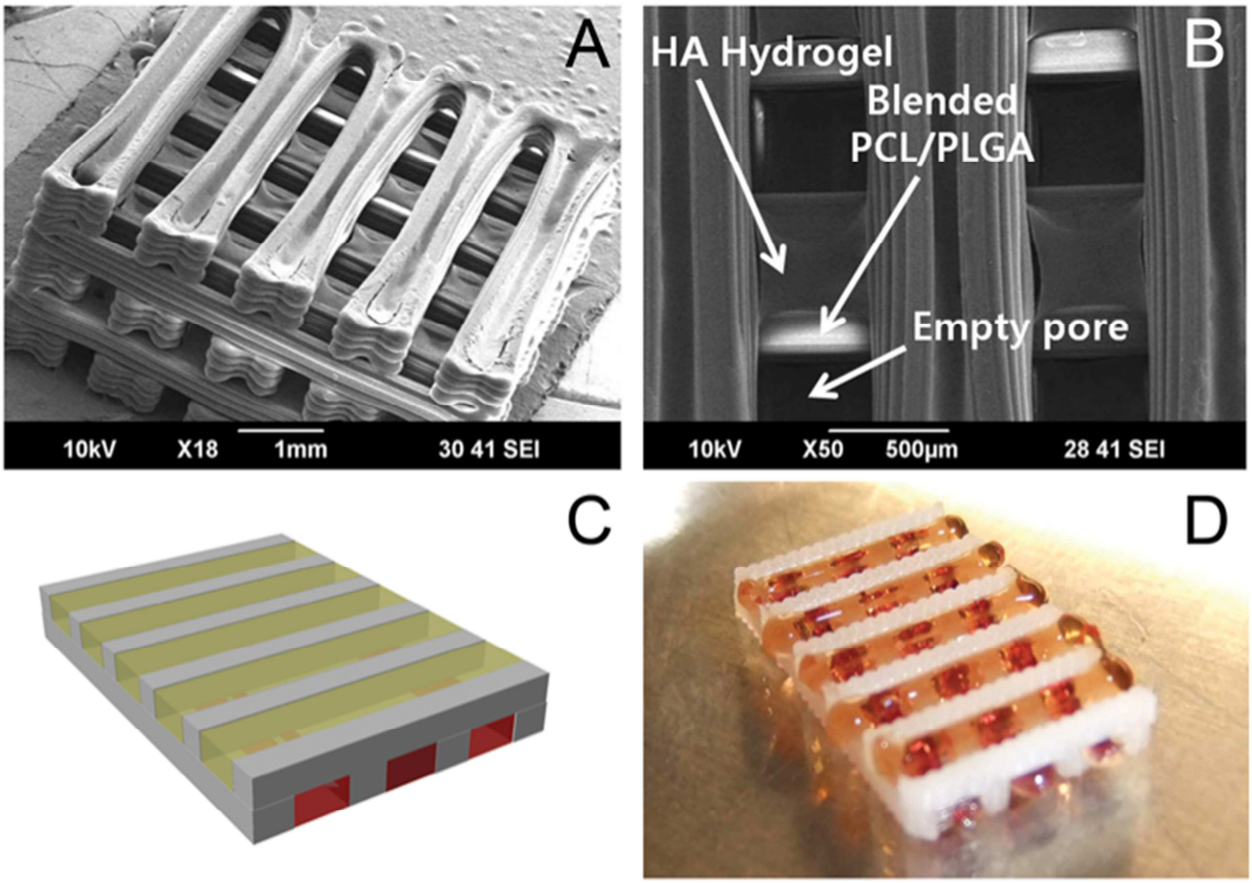

Figure 9. Examples of combined deposition of thermoplastic polymers and hydrogels. Scanning electron microscope images of a hybrid printed polycaprolactone (PCL)/ poly(lactic-co-glycolic acid) (PLGA) scaffold with infused HA hydrogel (A, B). A three-dimensional design (C) is translated to a deposition protocol, which uses (thermoplastic) PCL and alginate hydrogels (D). Reproduced with permission from Shim *et al.*[107] (A, B), Schuurman *et al.*[106] (C, D) and IOP Publishing. All rights reserved.

Table 1. Typical characteristics of three key dispensing approaches in biofabrication.

	Laser-induced forward transfer	Inkjet printing	Robotic dispensing
Resolution	++	+	+/-
Fabrication speed	-	+/-	++
Hydrogel viscosity	+/-	-	+
Gelation speed	++	++	+/-

Table 2. Hydrogels applied for fabricating 3D-structures.

hydrogel	fabrication technique	polymer concentration (w/v)	gelation method	printing quality	cytocompatibility	reference
	laser-induced forward transfer					
alginate		2%	ionic	2	intermediate, day 10	[121]
		1%	ionic	a*	high, day 7	[109]
		1%	ionic	3	high, day 1	[122]
		2%/8%	ionic	1/2	not studied	[123]
	inkjet					
alginate	thermal	2%	ionic	2	not reported	[124]
	piezo	0.8%	ionic	2	high, day 0	[50]
alginate/collagen type 1	thermal	1%/0.3%	ionic	2	90%, day 7	[125]
collagen type 1	not reported	0.1%	thermal	1	migrating cells	[126]
fibrinogen/collagen type 1	thermal	1%/0.15%	enzymatic	a*	82%, day 7	[105]
poly(ethylene glycol) dimethacrylate	thermal	10%; 20%	photo (during print)	2	89%, day 1	[13]
	robotic dispensing					
agar	pneumatic	5%	thermal	2	not studied	[72, 127]
agarose	piston-driven	1.5%	thermal	3[b*]	95%, day 21	[54]
	piston-driven	5%	thermal	1	95%, day 7	[25]
	piston-driven	not reported	thermal (cooling of strand in needle)	3[d]*	not studied	[128]
agarose	pneumatic	4%	thermal	2[*b]	not studied	[55]
alginate	piston-driven	10%	ionic	2	89%, day 1	[63]
	piston-driven	2%	ionic	2	82%, day 3	[25]
	piston-driven	2%	ionic	2	75-94%, day 0	[11, 84, 129]
	pneumatic	1.5% - 3%	ionic	2 (3%)	85%, day 0 (1.5%)	[130]
	piston-driven	4%	ionic	2	not studied	[40]
	piston-driven	2%	ionic	c*	70%, day 3	[106]

	pneumatic	3.5%	ionic	c*	84%, day 0	[108]
	piston-driven	4%	ionic	c*	94%, day 7	[131]
	pneumatic	5%	ionic	1[*b]	not studied	[55]
	piston-driven	1%	ionic	2	not studied	[132]
alginate/fibrin	pneumatic	6.3%/?%	ionic/enzymatic	1	not studied	[127]
alginate/gelatin	piston-driven	7.5%/5%	thermal/ionic/chemical	2	95%, day 0	[133]
atelocollagen	pneumatic	3%	thermal	c*	95%, day10	[107]
collagen type 1	pneumatic	0.3%	thermal	2	86%, day 1	[27, 134]
	pneumatic	0.223%	pH (sodium bicarbonate)	2[*e]	not studied	[135]
	piston-driven	0.1%	thermal	1	migrating cells	[126]
gelatin	piston-driven	20%	thermal/chemical	2	95%, month 1	[136]
	piston-driven	20%	thermal/chemical	2/3	poor cell differentiation	[137]
	pneumatic	7%	thermal	2[*d]	not studied	[135]
	pneumatic	2%	extruded in gel phase at 20°C	2	not studied	[55]
gelatin methacrylamide	piston-driven	20%	thermal /photo	1	73%	[57]
gelatin/alginate	piston-driven	6%/5%	thermal/ionic	3	82%, day 7	[12]
gelatin/alginate/chitosan	piston-driven	15%/1.25%/2.5	enzymatic/ionic/chemical	2	proliferating cells, day 7	
gelatin/alginate/fibrinogen	piston-driven	15%/1.25%/0.5%	thermal / enzymatic/ ionic/ chemical	2	proliferating cells, day 7	[138]
gelatin/alginate/fibrinogen	piston-driven	2:1:1	thermal/ionic/enzymatic	2	differentiating cells	[139]
gelatin/chitosan	piston-driven	5%/0.5%	ionic/ chemical	2	98%, month 2	[140]
gelatin/chitosan	piston-driven	4.6%/0.4%	thermal	1	Not reported	[141]
gelatin/chitosan	piston-driven	9%/1%	thermal	2	85-97%	[141]
gelatin/fibrinogen	piston-driven	13.3%/3.3% 10%/5% 6.6%/6.6%	enzymatic	2	98%, day 0	[142]
gelatin/Hyaluronan	piston-driven	10%/0.5%	thermal/chemical	2/3	poor cell differentiation	[137]
gelatin methacrylamide/ hyaluronic acid	piston-driven	20%/2.4%	thermal/photo	3	82%, day 3	[57]
gelatin methacrylamide/gellan	piston-driven	10%/1.1%	ionic/ thermal/photo	3 [e]*	80%, day 3	[93]

hyaluronic acid/ hydroxyethyl-methacrylate-derivatized- dextran (dex-HEMA)	piston-driven	10%	photo	2	75%, day 3	[88]
hyaluronic acid methacrylate (HA-MA)/gelatin methacrylate (GE-MA)	piston-driven	1.2%/0.3%	photo (during print)	1	proliferating cells, day 7	[83]
hyaluronic acid methacrylate (HA-MA)	piston-driven	1.5%	photo (during print)	1	not studied	[83]
Lutrol F127	piston-driven	25%	thermal	3	2%, day 7	[25]
	pneumatic	30%	thermal	3	60%, day 0	[27]
	piston-driven	40%	thermal	3[d]*	not applicable	[74]
Lutrol	piston-driven	25%	thermal/photo	3	50%, day 3	[11, 84]
Matrigel	piston-driven	not reported	thermal	1	High viability	[143]
methylcellulose	piston-driven	4%	thermal	1	not reported	[25]
N- isopropylamid and polyethylene glycol)	pneumatic	10%	thermal	2	not studied	[144]
poly(ethylene glycol) diacrylate	pneumatic	25%	photo	1	not studied	[55]
poly(ethylene glycol) diacrylate/ alginate	piston-driven	20%/12.5%	photo (during print)	3	near 100%, day 21	[44]
p(HPMAm-lactate)-PEG	piston-driven	25-35%	thermal /photo	3	94%, day 1	[24]
tetraPAc	piston-driven	1-2%	michael addition	2[e]*	high, day 28	[95]

Printing quality rated on shape-fidelity scale:

1= low undefined structure

2= intermediate irregular pattern/fiber, 3D potential

3= high well-defined building material

**a = reinforced with solution electrospun fibers*

**b = submerged fabrication technique*

**c = reinforced with co-deposited thermoplastic polymer scaffold*

**d = hydrogel is sacrificial component, no aim for direct cell encapsulation*

**e = support component used*

Table 3. Viscosities of some hydrogel precursor solutions used for printing.

polymer	concentration % w/v	viscosity (Pa·s)	shear rate (s^{-1})	molecular weight (kDa)	reference
sodium alginate	2	0.9	100	100-500 (typical)	[65]
	3	2.0			
	5	6.4			
Lutrol F127	25	0.03	-	12	[74]
	30	1.5			
	35	26 600			
	40	>600 000			
PE	10	0.008	200-1300	3.35	[13, 145]
	20	0.017			
Gelatin	10	0.02	50	50-100	[67]
Hyaluronic acid	1.5	22	1	950	[95]
Collagen type I	0.3	10	0.1-100	115+230	[27, 134, 146]
GelMA/gellan	10/0.75	1	50	50-100/1000	[67]

Jos Malda *is an Associate Professor of Joint Regeneration at the Department of Equine Sciences at Utrecht University and the Department of Orthopaedics at the University Medical Center Utrecht. His research focuses on biofabrication and biomaterials design, in particular for the regeneration of (osteo)chondral defects.*

((Author bio(s), max. 75 words))

Dietmar W. Hutmacher is the Professor and Chair of Regenerative Medicine at the Institute of Health and Biomedical Innovation of QUT, where he leads the Regenerative Medicine Group. He is also a Hans Fischer Senior Fellowship, Institute for Advanced Studies, Technical University Munich.

Author Photograph(s) ((40 mm broad, 50 mm high))

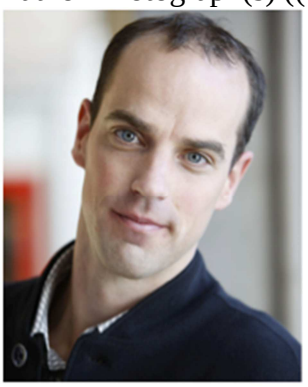


Hydrogels are attractive cell carriers for regenerative medicine as they recapitulate several features of the natural extracellular matrix. However, biofabrication of three-dimensional complex, tissue-like structures with high shape fidelity dictates narrow boundaries for the physical properties of the hydrogels applied. This review focuses on strategies and new developments that address these physicochemical challenges.

Keywords: Hydrogels; Tissue Engineering; Biomedical Applications; Stimuli-Responsive Materials; Inkjet Printing

J. Malda*, J. Visser, F. P. Melchels, T. Jüngst, W. E. Hennink, W. J.A. Dhert, J. Groll, and D. W. Hutmacher*

Engineering Hydrogels for Biofabrication

ToC figure:

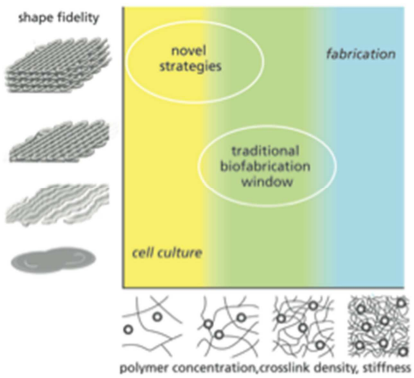
shape fidelity
novel strategies
fabrication
traditional biofabrication window
cell culture
polymer concentration,crosslink density, stiffness